Unbalance Voltage Compensation Using Power Electronics Interfaced DG

by

Jinghang Lu

A thesis submitted in partial fulfillment of the requirements for the degree of

Master of Science

Energy Systems

Department of Electrical and Computer Engineering
University of Alberta

© Jinghang Lu, 2014

Abstract

With the increasing application of renewable energy systems, many Distributed Generation (DG) systems have been connected to power systems. Power electronic converters are usually used as effective interfaces of DG unit. These interfaces convert either DC or non-grid AC voltages of DGs to the grid compatible AC voltage.

On the other hand, unbalanced voltage caused by local load adversely affects distribution network's power quality. Therefore, operating DG unit under unbalanced voltage and using grid-interfacing converter to improve the grid's power quality is becoming an important research topic

This thesis first reviews grid-interfacing converter control methods that provide various flexible operations under unbalanced voltage. Furthermore, to reduce the impact on converter dc link due to unbalanced current injection, two DG control strategies for voltage unbalance compensation are proposed. Their validity was verified by Matlab/Simulink and a lab prototype.

Preface

This thesis is an original work by Jinghang,Lu. Chapter 2 was a reviewed part, which was published in IEEE Transaction Papers. Chapter 3 and Chapter 4 of this thesis have been accepted as J.Lu, F.Nejabatkhah, Y. W. Li and Bin Wu “DG Control Strategies for Grid Voltage Unbalance Compensation”, in *Conf. Rec. IEEE Energy Conversion Congress and Exposition.* Farzam. Nejabatkhah assisted with method realization. Dr. Yunwei Li was the supervisory author and was involved with concept formation and manuscript composition. Dr. Bin Wu from Ryerson University was collaborator, who contributed to the manuscript composition.

Acknowledgement

I would like to express my sincere gratitude to Dr. Yunwei (Ryan) Li for his financial support. This research and dissertation would not have been possible without his patient guidance and great supervision.

I also would like to thank my parents for supporting me in many different ways during my study in Canada.

Finally I also thank students in Dr Li's research group, Ye Zhang, Xiaohan Wen, Yujuan Lian. Especially, thank Farzam for his fruitful discussion and assistance that helped improve the work.

Contents

List of Tables

List of Figures

Chapter 1 Introduction

Over the last few decades, renewable energy sources have been attracting great attention due to the limitations and adverse environmental effects of fossil fuels [1]. Power electronics grid-interfacing converters play a key role that enables the efficient and flexible interconnection of renewable energy sources to electric power systems. However, with the increasing tendency to connect unbalanced load to the grid, the voltage unbalance problem is severely degrading the distribution system's power quality [2]. This problem presents many challenges for researchers seeking techniques for controlling grid-interfacing converter. Therefore, the power quality enhancement of grid by using power electronics grid-interfacing converter is becoming a hot research field where ancillary unbalanced voltage compensation is integrated with the control of converter besides the primary power delivery function [3].

1.1 Voltage Unbalance Review

Due to the increasing number of local loads that are being connecting to power systems, power distribution systems are facing many power quality problems, such as voltage unbalance, harmonics, and voltage flicker [4], among which the voltage unbalance issue especially needs to be drawn attention. As voltage unbalance can trip of equipment, interrupt production, and jeopardize the power system operation. Therefore, in the next few sections, the details of this issue will be discussed.

1.1.1 Causes of Voltage Unbalance

One issue that utility companies are facing is unbalanced voltage in the distributed network. Unbalanced voltage indicates unequal voltage magnitudes at

the fundamental system frequency (under voltage and over-voltage), fundamental phase angle deviation and unequal levels of harmonic distortion [5]. One major cause of voltage unbalance is the connection of unbalanced loads (mainly single-phase loads connected between two phases or one phase and the neutral). Unbalance voltage can occur in rural electric power systems with long distribution lines, as well as in large urban power systems where single-phase demands, such as lighting loads, are imposed by large commercial facilities [6]. Another cause of unbalance is single phase traction and electric transit and railroad systems [7]. Asymmetrical transformer winding impedance, open wye and open delta transformer banks, and asymmetrical transmission impedance can also cause considerable imbalance in the power system [4]. In the industry, unbalanced voltage can also be caused by unbalanced equipment. For example, motor impedance unbalance, which is becoming increasingly severe, is caused by unbalanced heating of a motor [8]. Motor unbalance is usually caused during manufacturing by creating an unequal number of turns in the winding or asymmetrical stator. Recently, with the increasing use of adjustable speed drives (ASD), voltage unbalance problems have become quite severe, especially when a large number of single phase ASDs are employed. Therefore, balancing the voltage when incorporation of ASDs and power electronics are distorting the grid has become a major challenge.

In DG systems, the unbalanced grid voltage is usually caused by the connection of a single-phase DG system and an unbalanced load to a three-phase DG system [1]. Ideally, a large number of single-phase DG systems will be evenly distributed among the three-phase distribution lines, and consequently, no unbalanced voltage will occur in the grid. However, in practice, any difference in the distribution will cause grid voltage imbalance.

1.1.2 Voltage Unbalance Impact

Unbalanced voltage can have an adverse effect on equipment and power systems. Under unbalanced conditions, the grid suffers more losses and heating effects and become less stable. Voltage unbalance can also cause capacity losses, transformer overloading, motor overheating, nuisance tripping of protected devices, and malfunction in sensitive equipment [9]. Overall, the negative effect of voltage unbalance can reduce efficiency and decrease lifespan of equipment.

1.1.2.1 Voltage Unbalance Effects on Motor

Unbalanced voltages have negative effects on induction motors because the unbalanced voltage can be separated into positive sequence voltage, negative sequence voltage and zero sequence voltage by using the symmetrical component extraction method [10]. However, zero sequence voltage does not exist in machines because motors normally use either delta connection wire or undergrounded wye, so a zero sequence component has no path to formulate a circuit. Therefore, balanced systems contain only the positive and negative sequence component of the voltage, current, and impedance.

Hence, unbalanced motor voltage can be divided into opposing voltage sequence voltage, i.e., “abc” and “acb”, respectively. The positive sequence voltage leads to a desired positive torque, whereas negative sequence voltage leads to a reversing torque, which is caused by an air gap flux rotating against the rotation of the rotor. The unwanted torque can cause speed reduction and torque pulsation, and even increase the motor noise [11]. Moreover, the negative sequence current generated by the negative sequence voltage due to the motor’s impedance can cause machine loss and even high temperature [11].

Another effect of voltage unbalance is motor damage from excessive heat. Voltage unbalance can create a current unbalance 6 to 10 times the magnitude of

the voltage unbalance. In turn, a current unbalance produces heat in the motor windings that degrades the motor insulation, causing cumulative and permanent damage to the motor [5, 11]. This scenario results in expensive facility downtime due to motor failures.

Fig.1. 1 below shows the relationship between voltage unbalance and temperature rise, which increases by approximately twice the square of the percentage of the voltage unbalance [5].

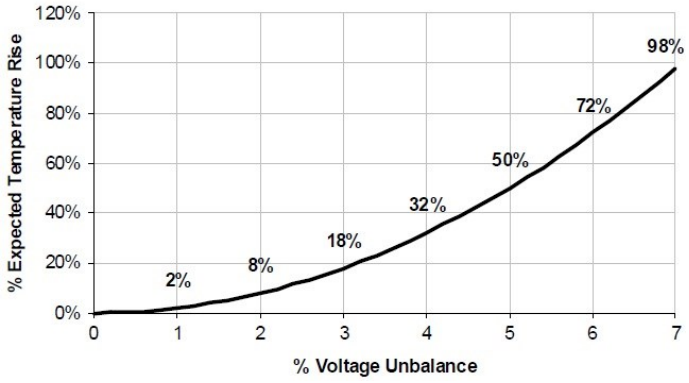

Fig.1. 1Voltage Unbalance and Temperature Rise [5]

1.1.2.2 Voltage Unbalance Effects on Sensitive Loads

Voltage unbalance can cause severe problems for sensitive loads as well. Voltage unbalance in the terminal of a load affects the equipment's normal operation. Particularly sensitive loads such as servers, computer centers, and communication equipment may fail to work properly due to insufficient voltage for regulation. Shutdown or long restart time of sensitive loads can quickly result in losses of several hundred thousand dollars, especially in key industries. Sensitive loads such as servers, computer centers, and communication equipment are commonly protected against voltage imbalance by using dynamic uninterrupted power systems (UPS) and flywheel buffer systems [4].

1.1.2.3 Voltage Unbalance Effects on Power Electronics Load

In systems with a large fraction of load formed by either single-phase or three-

phase rectifier, a long and deep voltage unbalance will trip a large part of electronic loads. The equipment which does not trip will undertake a smaller current from the supply because the dc bus voltage is larger than the peak of the ac voltage. For three-phase rectifiers, under unbalanced voltage, the largest current flows between the two phases with the largest voltage difference. The current to the three phase rectifiers will contain non-characteristic harmonics. The three-phase controlled rectifiers will experience a longer communication period because the source voltage is lower during the unbalanced voltage [4].

1.1.3 International Standards in Voltage Unbalance

Two methods have been proposed for determining the level of voltage unbalance.

The voltage unbalance in percentage is defined by the National Electrical Manufacturers Association (NEMA) in Standards Publication no. MG 1-1993 as [12]:

$$\%\text{Unbalance} = \frac{\text{Maximum Deviation from Average}}{\text{Average of Three Phase to Phase Voltage}} \times 100 \qquad (1\text{-}1)$$

Note that the line voltages are used in this NEMA standard as opposed to the phase voltages. When the phase voltages are used, the phase angle unbalance is not reflected in the % unbalance, and therefore phase voltages are seldom used to calculate the voltage unbalance.

Another index used in European standards to indicate the degree of unbalance is the voltage unbalance factor (VUF), which is the ratio of the negative sequence voltage to the positive sequence voltage represented as [13]

$$\%\text{VUF} = \frac{V_2}{V_1} \times 100 \qquad (1\text{-}2)$$

where V_1 and V_2 are the positive and negative sequence voltages, respectively, and can be obtained by using symmetrical components.

Meanwhile, different standards exist for limiting the voltage unbalance. The

American National Standard for Electric Power Systems and Equipment. ANSI C84.1 [14] recommends that "electric supply systems should be designed and operated to limit the maximum voltage unbalance to 3% when measuring the electric-utility revenue meter under no-load conditions" while the International Electrotechnical Commission (IEC) recommends that the maximum voltage unbalance of electrical supply systems should be limited to 2% [15].

The National Equipment Manufacture Association (NEMA) suggests that motors should give a rated output for 1% of the voltage unbalance per NEMA MG-1-1998 [16]. By limiting the voltage unbalance to 1%, this standard is more rigorous than ANSI C84.1. Moreover, some motor manufactures have tried to require less than 5% current unbalance for a valid warranty. NEMA MG-1 states that 1% of voltage unbalance can generate 6-10% current unbalance, therefore, motor manufacturers are required to adhere to more stringent voltage unbalance standards.

According to IEEE Std 141-1993, "IEEE Recommended Practice for Electric Power Distribution for Industrial Plants" and IEEE Std.241-1990, "IEEE Recommended Practice for Electric Power Systems in commercial buildings", some equipment may experience problems if the voltage unbalance is beyond 2 or 2.5%. However, according to IEEE Std 1527.2-2008 [17], the voltage unbalance should be limited to 5% when distributed generation is connected to a low voltage system.

1.2 Conventional Methods for Unbalanced Voltage Compensation

Voltage unbalance problems are either introduced by unbalanced distribution of loads or come from the upstream grid. Hence, compensation systems for unbalanced voltage should be installed in between the grid and the asymmetrical load. Conventionally, the installation of a generator near a sensitive load is an

effective way to keep the voltage up during a remote unbalanced voltage drop [18]. An alternative way is to choose an appropriate distribution transformer to prevent voltage unbalance, particularly in balancing the open wye and open delta transformer banks [19]. However, open wye-open delta banks can greatly jeopardize the unbalance of the primary system as it converts zero sequence voltage into secondary system negative sequence voltage. In addition, unbalanced compensation can be achieved by using a passive power filter which balances the load impedance [20].

With the power electronic development, two types of compensators with fully controlled power electronic devices are adopted to alleviate the unbalanced voltage amplitude. The use of shunt-connected converter is an effective way to minimize voltage unbalance (see in Fig.1. 2). Such a shunt converter can act as a shunt Active Power Filter (APF) or shunt SATCOM. In [21], the voltage at the grid connection point is regulated by injecting reactive current from the shunt active power converter, which introduces a voltage drop across the grid impedance. However, voltage compensation will be not effective when the grid-impedance is either too low, or is dominantly resistive and needs an injection of active power.

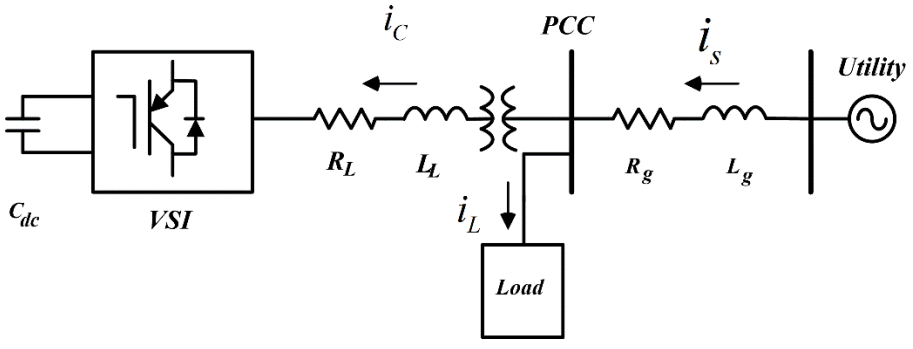

Fig.1. 2 Structure of Shunt Connected Converter

The alternative way to compensate the unbalanced voltage is to use a series-connected converter, as is shown in Fig.1. 3, where negative-sequence or zero

sequence voltage is injected to compensate the unbalanced component of grid voltage. Such a series-connected converter can be series Active Power Filter (APF) and Dynamic Voltage Restorer (DVR). However, a series-connected converter has to provide active power when a three-phase load is asymmetrical due to the active power generated by symmetrical sequence components.

Therefore, the shunt and series connected converter are mainly used for power quality improvement, and are specifically designed to compensate for certain power quality problems by injecting current or voltage into the system.

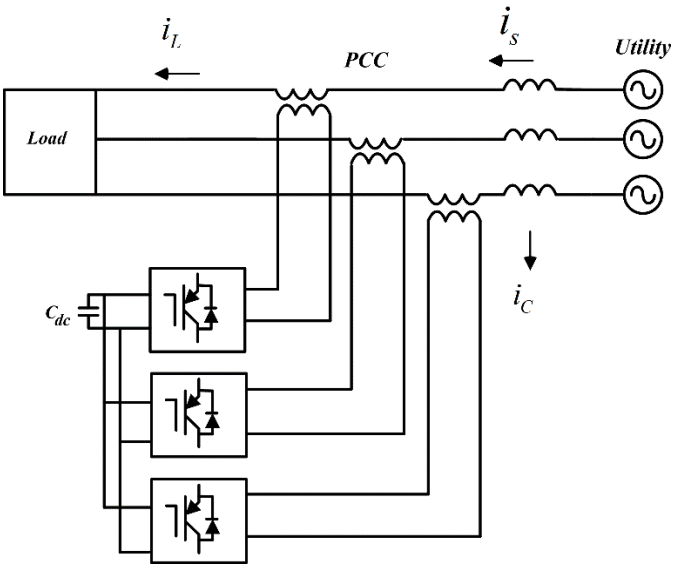

Fig.1. 3 Structure of Series Connected Active Filter

For dealing with other power quality problems other than unbalanced voltage, the unified power quality conditioner (UPQC) have been proposed. A typical UPQC is shown in Fig.1. 4, where two voltage source converters share a common dc bus. One converter is in series with the distribution feeder while the other is in parallel with the same feeder. Load 2 on the left side needs balanced and sinusoidal voltage. In this structure, the purpose of the series converter is to eliminate harmonics between the grid and the local distribution network. Moreover, the series converter is able to compensate for the voltage imbalance. The main purpose of a

parallel converter is to absorb the current harmonics to compensate for negative sequence current and regulate dc bus voltage [22].

In this way, UPQC can protect the voltage of load 2 from unbalance voltage and harmonics occurring in the source of the distribution network. However, when voltage of load bus collapses to a low value, the parallel converter is unable to draw the amount of power required to recharge the dc capacitor. In this case, energy storage devices such as batteries or super capacitors must be connected to the dc link in order to provide voltage support.

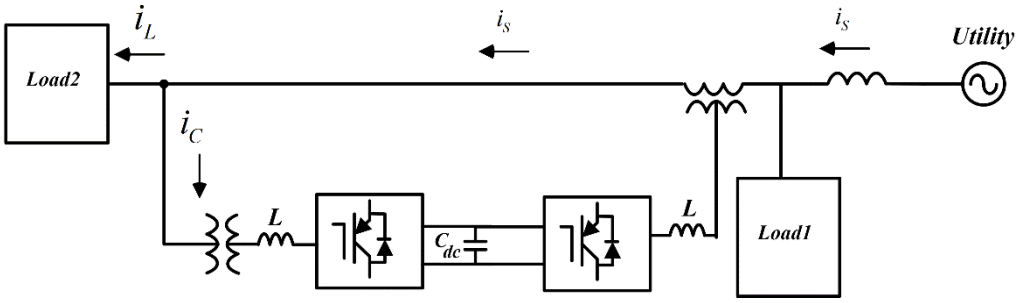

Fig.1. 4 Structure of Unified Power Quality Conditioner

1.3 Using DG Grid-interfacing Converter in Unbalanced Voltage Mitigation

Distributed generation (DG) refers to an electrical power source generated from renewable energy (RE) resources such as wind, photovoltaic, clean alternative energy (AE) generation such as fuel cells and microturbines, as well as the traditional rotational machine based technologies such as diesel generators that connected to the distributed network [23, 24].

Most DG systems are installed in distributed network where they enables bi-directional power flow instead of traditional one-way power flow from high voltage network to low voltage network in the centralized power system.

With the increasing installation of DG systems, the unbalanced load and the

nonlinear load are connected to the grid, so utilities are struggling to maintain their power quality. As a result, the increasing demand for DG control of unbalanced voltage and harmonics has prompted researchers to seek more effective ways to improve the grid voltage performance.

Several different controllers for current or voltage regulation have been adopted to deal with unbalanced voltage and harmonics in the grid. First, the proportional-integral (PI) controller is widely used in conjunction with dq control structure. This control structure enables control variable to transform from their natural *abc* frame to the dq frame. As a consequence, the control variables becomes dc signals [25]. Specifically, this control structure needs information about phase angle of the utility voltage to perform the transformation [26]. However, if the controller is immune to grid voltage harmonic distortion, harmonic compensator has to be designed at each harmonic order, and this requirement greatly increases the complexity of the control algorithm. On the other hand, many power converters have been designed with proportional resonant (PR) controllers. Their use has been demonstrated to be an effective method for controlling inverter systems under unbalanced and harmonic grid conditions [25]. Another method to control the inverter is to use dead-beat controller, which is suitable for microprocessor-based implementation. This controller has theoretically a very high bandwidth, hence, its tracing of sinusoidal signals is quite good. However, since dead beat controller is developed on the basis of model. It is sensitive to model and parameter mismatch [26].

To compensate for the distribution system unbalanced voltage, installing an additional filter is not advisable due to the cost concerns. Alternatively, distribution system voltage unbalance compensation using DG system is becoming an interesting topic, where the ancillary voltage imbalance compensation capability is

integrated into the DG's primary power delivery function by modifying DG's control reference [27]. This method is preferable for power electronic interfaced DG system, where the power electronic interface can be flexibly controlled to provide such ancillary functions.

Using a single DG system for voltage unbalance compensation by injecting a negative sequence current has been proposed in [28]. By applying this method, the line current becomes balanced under an unbalance load. However, under voltage unbalance deterioration, the capability to inject negative sequence current is limited.

To overcome the weakness of aforementioned method, several papers have been proposed using multiple DG systems with droop control or secondary control to compensate for unbalanced voltage [29]-[31]. Paper [29] proposed a droop control technique with multiple DGs for voltage unbalance compensation. The paper [30] proposed a voltage and frequency control strategy for islanded operation of dispatched electronically coupled distributed-resource unit. When the power quality at the point of common coupling (PCC) is the main concern due to the sensitive loads connecting. paper [31] proposed the microgrid secondary control to compensate for the voltage unbalance at PCC in an islanded microgrid.

The use of wind turbine converters to compensate for unbalanced voltage has also been investigated as well [32]. In paper [32], a series converter is connected to double-fed induction generator to mitigate the unbalanced voltage with phase jumps by using classical optimization. The author uses the objective function with constraints for mitigating the unbalanced voltage, thus, the real power injection by series converter of DFIG is minimized.

Other method that deals with harmonic voltage compensation can also be implemented for voltage unbalance mitigation and reactive power compensation. In [33]-[34], two DG control methods are considered and associated power quality

compensation strategies are implemented. In [35], a proportional integral repetitive control scheme is proposed to mitigate the levels of harmonic and unbalanced voltage at the stator terminal of DFIG. Such methods for dealing with the harmonic and unbalanced voltage simultaneously can also be found in paper [34].

Voltage unbalance compensation can lead to active power oscillation at PCC. This problem can, in turn, cause DC link ripple, resulting in adverse effects on the DG operation or even system instability. However, the existing methods have never addressed this issue.

1.4 Research Goal and Thesis Layout

The goal of this thesis is to develop unbalanced compensation strategy for the grid-interfacing power electronic DG system where voltage quality improvement and flexible power control are combined together, minimizing the impact on DC link ripple and DG operation. To achieve this goal, the main research focused on the following.

First, studies were carried out on flexible power control strategies based on a fast current controller and a reconfigurable reference current selector when the DG operates under grid unbalanced voltage. Several existing strategies in the literature for the DG's output reference current generations are studied and compared in Chapter 2.

Moreover, two separate control strategies for voltage unbalanced compensation under unbalance load conditions are proposed in Chapter 3 to limit the active power oscillation caused by unbalanced voltage. In the first method, the active power oscillation is cancelled. However, the level of unbalanced voltage compensation cannot be controlled directly by this method. Therefore, a second control strategy is proposed to minimize the active power oscillation (instead of completely

cancelling it) by using an adjustable unbalanced voltage compensation according to the DG's available capacity.

Furthermore, to ensure the high performance of the DC link voltage and DG output current control, the proposed control strategies include high performance techniques for voltage detection and synchronization in disturbed voltage. In this fast and accurate detection method, three fundamental functional blocks make up the detector, (1) the quadrature-signals generator (QSG), (2) the positive sequence calculator (PSC), and (3) the phase locked-loop (PLL), meanwhile, the dual second order generalized integrator (DSOGI) is implemented to improve the voltage unbalance detection. The details for design of controller are also presented in this chapter.

Finally, a laboratory hardware prototype is used to verify all the control methods studied in this thesis. The experimental results are provided and discussed in Chapter 4.

The conclusions from the research and some suggestion for future research are presented in Chapter 5.

Chapter 2 Flexible power control of DG under unbalanced voltage

2.1 Introduction

Last few years have witnessed the development of distributed power generation systems, especially renewable energy such as wind turbine and solar power have made a great contribution to the total amount of energy production in the world. Although the energy production of wind turbine and solar power have attractive market, the control of these power system is a challenge and the increased distributed power generation can cause instability and even outrage in the power system [36].

In order to maintain the stability of power system when large amount of distributed power system integrates into the grid, transmission operators are requested to follow the strict demands with regard as distributed power system interconnecting to the utility grid. Among all the demands, distributed power system are requested to work properly under voltage unbalance at point of common coupling (PCC). Therefore, the unbalanced voltage influences on the control of distributed power generation system need to be investigated.

In this chapter, several control strategies that could be adopted by distributed generation (DG) system will be reviewed under unbalanced voltage at PCC [26]. First, Instantaneous power theory will be presented, followed by different control strategies under unbalanced voltage in the utility. Finally, the simulation results will be illustrated to demonstrate the validity of control algorithm.

2.2 Current control strategies under unbalanced voltage at PCC

In this section, instantaneous power theory is first reviewed [37]. Then, instantaneous power calculation based on symmetrical voltage sequence is developed. Finally, a variety of control strategies are designed.

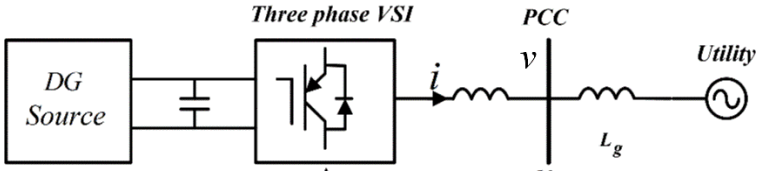

Fig.2. 1 A distributed generation inverter operating connecting to grid

In a three phase inverter system shown in Fig.2.1, instantaneous active power and reactive power at the utility connection point are given by [38].

$$p = v \cdot i = v_a i_a + v_b i_b + v_c i_c \tag{2-1}$$

where the operator "·"denotes the dot product of two vectors.

When active power is expressed in symmetrical component, there will be the following expression:

$$p = v^+ \cdot i^+ + v^+ \cdot i^- + v^- \cdot i^+ + v^- \cdot i^- = P + \tilde{p} \tag{2-2}$$

where v^+, v^-, i^+, i^- are positive and negative sequence component of voltage and current vectors, and P and $\tilde{p}$ are average term and oscillatory term of active power.

Meanwhile, the instantaneous reactive power can be defined as cross-product between v and i, and can be calculated by means of the following dot product,

$$q = v_\perp \cdot i \tag{2-3}$$

where $v_\perp$ is 90 degree lagging vector compared to vector v.

When the reactive power is expressed in symmetrical component, it will be calculated as follows:

$$q = v_\perp \cdot i = (v_\perp^+ + v_\perp^-) \cdot (i^+ + i^-) \tag{2-4}$$

$$q = v_\perp^+ \cdot i^+ + v_\perp^- \cdot i^- + v_\perp^+ \cdot i^- + v_\perp^- \cdot i^+ = Q + \tilde{q} \tag{2-5}$$

where the Q and $\tilde{q}$ are average and oscillatory terms of reactive power,

respectively

In the following, several different control strategies for determining the current vector (i^*) will be reviewed and discussed when delivering active and reactive power into the grid under unbalanced grid voltage conditions. The performance of these control strategies for calculating reference currents will be discussed and compared since these control strategies will provide different features for grid-interfacing DG system [25].

2.2.1 Instantaneous active-reactive control (IARC)

From the instantaneous active power and reactive power theory, current vector i which aligns with voltage vector v wil give rise to active power, current vector i aligned with $v_\perp$ will generate reactive power. Therefore, the following expression can be concluded according to this concept. In order to deliver constant active power ($p = P^*$) and constant reactive power ($q = Q^*$), the current reference based on instantaneous power theory could be calculated as follows [39]:

$$i_p^* = gv \tag{2-6}$$

$$i_q^* = bv_\perp \tag{2-7}$$

where i_p^* and i_q^* are considered as active and reactive current vectors respectively, g represents instantaneous conductance and b represents instantaneous susceptance.

The product of current and voltage vector can give rise to a certain amount of power *P* and *Q* with grid voltage v. Therefore, there will be the following equations:

$$i_p^* \cdot v = gv \cdot v = P \Longrightarrow g = \frac{P}{|v|^2} \tag{2-8}$$

$$i_q^* \cdot v_\perp = bv_\perp \cdot v_\perp = Q \Longrightarrow b = \frac{Q}{|v|^2} \tag{2-9}$$

So, the reference current vectors to deliver the P and Q power to the grid is expressed as :

$$i_p^* = \frac{P}{|v|^2} v \tag{2-10}$$

$$i_q^* = \frac{Q}{|v|^2} v_\perp \tag{2-11}$$

where i_p^* is the active power component of reference current vector and i_q^* is the reactive power component of vector. Therefore, the final reference can be calculated by just adding (2-10) and (2-11)

$$i^* = i_p^* + i_q^* \tag{2-12}$$

In (2-10) and (2-11)，the norm of grid voltage vector $|v|^2$ can be calculated as follows [39]:

$$|v|^2 = v_a^2 + v_b^2 + v_c^2 = v_\alpha^2 + v_\beta^2 = v_d^2 + v_q^2 \tag{2-13}$$

Under balanced sinusoidal conditions, the current injecting to the grid is perfectly sinusoidal, because the module of the voltage $|v|$ and g and b are constant. However, when voltage unbalance occurs, voltage at PCC are separated into positive sequence and negative sequence voltages. And the module of $|v|^2$ has oscillation at twice the fundamental grid frequency, i.e.

$$|v|^2 = |v^+|^2 + |v^-|^2 + 2|v^+||v^-|\cos(2wt + \emptyset^+ - \emptyset^-) \tag{2-14}$$

where $\emptyset^+$ and $\emptyset^-$ are positive and negative initial phase angles of v^+ and v^-.

When the expression is replaced in the denominator of (2-10) and (2-11), the reference current i_p^* and i_q^* are not sinusoidal and contains high order harmonics, resulting in distorted reference signals. The drawback of this control strategy is that it has the possibility to inject distorted current. In the high power grid-connected converter, injecting harmonics is limited where it can give rise to additional problems, such as excitation of resonance or deterioration of the grid voltage.

Therefore, although IARC has the obvious advantage of power controllability, the application of IARC will not be suitable for generating reference current because the low quality of injecting current may be not acceptable when the

unbalanced voltage occurs in the grid. Hence, instantaneous power calculations based on symmetrical sequence components are derived in the following.

2.2.2 Positive and Negative Sequence Control (PNSC)

This strategy deals with calculation of reference current vector, including positive and negative sequence current that can eliminate the oscillatory instantaneous power that is injected into the grid.

First, it is assumed that reference current injecting into the grid is expressed as:

$$i^* = i^{*+} + i^{*-} \tag{2-15}$$

where i^{*+} and i^{*-} represent positive and negative sequence reference current

It is initially assumed that only active power is delivered into the grid, and the active power at PCC is free of oscillation [25]. Considering the two constrains, there exists the following expression:

$$v^+ \cdot i_p^{*+} + v^- \cdot i_p^{*-} = P \tag{2-16}$$

$$v^+ \cdot i_p^{*-} + v^- \cdot i_p'^{*+} = 0 \tag{2-17}$$

$$v^+ \cdot i_p^{*-} = -v^- \cdot i_p^{*+} \Longrightarrow |v^+|^2 \cdot i_p^{*-} = -v^+ \cdot i_p^{*+} \cdot v^-$$

$$\Longrightarrow i_p^{*-} = -\frac{v^+ \cdot i_p^{*+}}{|v^+|^2} v^- \tag{2-18}$$

Therefore, the following equation can be found by substituting and regrouping terms :

$$P = v^+ \cdot i_p^{*+} \left(1 - \frac{|v^-|^2}{|v^+|^2}\right) \tag{2-19}$$

And the positive sequence reference current is derived as:

$$i_p^{*+} = \frac{P}{|v^+|^2 - |v^-|^2} v^+ \tag{2-20}$$

Finally, the positive and negative reference current is given by

$$i_p'^* = g^{\pm}(v^+ - v^-), g^{\pm} = \frac{P}{|v^+|^2 - |v^-|^2} \tag{2-21}$$

Similarly, to determine the reference current for the reactive power, we have the

following equation:

$$v_{\perp}^{+} \cdot i_{q}^{*+} + v_{\perp}^{-} \cdot i_{q}^{*-} = Q \tag{2-22}$$

$$v_{\perp}^{+} \cdot i_{q}^{*-} + v_{\perp}^{-} \cdot i_{q}^{*+} = 0 \tag{2-23}$$

From the above equation, the current reference for the reactive power is the following expression:

$$i_{q}^{*} = b^{\pm}(v_{\perp}^{+} - v_{\perp}^{-});\ b^{\pm} = \frac{Q}{|v^{+}|^{2} - |v^{-}|^{2}} \tag{2-24}$$

Therefore, the final reference current is calculated as:

$$i^{*} = i_{p}^{*} + i_{q}^{*} = g^{\pm}(v^{+} - v^{-}) + b^{\pm}(v_{\perp}^{+} - v_{\perp}^{-}) \tag{2-25}$$

In the PNSC control strategies, the positive and negative sequence currents injecting into the grid is written as the active and reactive component as follows:

$$i^{+} = i_{p}^{+} + i_{q}^{+} \tag{2-26}$$

$$i^{-} = i_{p}^{-} + i_{q}^{-} \tag{2-27}$$

So the instantaneous active and reactive power delivered by the converter is expressed as:

$$p = \underbrace{v^{+}i_{p}^{+} + v^{-}i_{p}^{+}}_{P} + \underbrace{v^{+}i_{q}^{+} + v^{-}i_{q}^{-}}_{0} + \underbrace{v^{+}i_{p}^{-} + v^{-}i_{p}^{+}}_{0} + \underbrace{v^{+}i_{q}^{-} + v^{-}i_{q}^{+}}_{\tilde{p}} \tag{2-28}$$

$$q = \underbrace{v_{\perp}^{+}i_{q}^{+} + v_{\perp}^{-}i_{q}^{-}}_{Q} + \underbrace{v_{\perp}^{+}i_{p}^{+} + v_{\perp}^{-}i_{p}^{-}}_{0} + \underbrace{v_{\perp}^{+}i_{q}^{-} + v_{\perp}^{-}i_{q}^{+}}_{0} + \underbrace{v_{\perp}^{+}i_{p}^{-} + v_{\perp}^{-}i_{p}^{+}}_{\tilde{q}} \tag{2-29}$$

In both (2-28) and (2-29) third and fourth term are cancelled, as the dot product of two terms with same sequence and 90 degree shifted equals zero. The fifth and sixth term in (2-28) and (2-29) are also zero considering the equation of (2-17) and (2-23), where both oscillating terms are set to be zero when calculating the reference current. As is seen from (2-28) and (2-29), when PNSC strategy is implemented, the instantaneous active and reactive power p and q differ from the reference P and Q due to the interaction between in-quadrature voltage and current with different sequences.

However, when one of the power reference is null, i.e. Q is set to be zero, the

performance of instantaneous power at PCC is slightly different. Active power oscillation is cancelled, this is due to the fact that oscillatory component in the $\tilde{p}$ depends on reactive power component i_q^- and i_q^+, whose reference is zero[39].

2.2.3 Average Active-Reactive Control (AARC)

As is mentioned previously, when unbalanced voltage occurred in the grid, the reference current using IARC strategies present harmonics in the waveform because of oscillation terms in g and b . Since *P* and *Q* is assumed to be constant, such harmonics come from effect of the second-order component of $|v|^2$ on the calculation of the instantaneous conductance and susceptance [25]. Therefore, if the second-order component of $|v|^2$ is cancelled out, the harmonics will be eliminated as well. To achieve this objective, the average active-reactive control strategy calculate average value of conductance and susceptance throughout one period, so the active and reactive reference current is calculated as [39]:

$$i_p^* = Gv; G = \frac{P}{V_\Sigma^2} \tag{2-30}$$

$$i_q^* = Bv; B = \frac{Q}{V_\Sigma^2} \tag{2-31}$$

where V_Σ is rms value of the grid voltage, and is defined as:

$$V_\Sigma = \sqrt{|v^+|^2 + |v^-|^2}$$

Since *G* and *B* are constant in this control strategy, there is no oscillation in the reference current. Considering active power injection, the current injecting to the grid has the same direction with grid voltage. Therefore, there will be no reactive power component showing in the grid. However, instantaneous power sending to the unbalanced grid will not equal to P but will be present by:

$$p = i_p^* \cdot v = \frac{|v|^2}{V_\Sigma^2} P = P + \tilde{p} \tag{2-32}$$

where $\tilde{p}$ is the oscillatory term adding to the average value P

So, the actual instantaneous power delivered to the unbalanced grid is written as :

$$p = P\left[1 + \frac{2|v^+||v^-|}{|v^+|^2+|v^-|^2} cos(2wt + \varphi^+ + \varphi^-)\right] \quad (2\text{-}33)$$

where φ^+ and φ^- are the phase angles of the positive and negative sequence voltage v^+ and v^-

In the same way, reactive current has the same direction with in-quadrature voltage $v_\perp$. As discussed in the active power scenario, the actual reactive power consists of constant term and oscillatory term as well and can be written as:

$$q = v_\perp \cdot i_q^* \quad (2\text{-}34)$$

$$q = Q\left[1 + \frac{2|v^+||v^-|}{|v^+|^2+|v^-|^2} cos(2wt + \varphi^+ - \varphi^-)\right] \quad (2\text{-}35)$$

After acquiring the equation for p and q in (2-33) and (2-35), it can be observed that the instantaneous reactive power delivered into grid will be zero, if just active power is injected into grid by AARC strategy. Likewise, if only reactive power delivers into the grid, active power will be zero.

2.2.4 Balanced Positive Sequence Control (BPSC)

Considering the previous AARC control strategy, there is possibility to change the conductance and susceptance to calculate the reference current for obtaining other objectives. In the balanced positive sequence control strategy (BPSC), the goal is to inject only balanced positive sequence sinusoidal current. So the reference current for the BPSC strategy [38]is written as:

$$i_p^* = G^+ v^+; G^+ = \frac{P}{|v^+|^2} \quad (2\text{-}36)$$

$$i_q^* = B^+ v^+; B^+ = \frac{Q}{|v^+|^2} \quad (2\text{-}37)$$

The reference current consists of balanced sinusoidal positive waveform. Under unbalanced operating conditions, the instantaneous active and reactive power

delivered into the grid will contain two parts: average power term and oscillatory power term, i.e

$$p = i_p^* \cdot v = v^+ i_p^* + v^- i_p^* = P + \tilde{p} \tag{2-38}$$

$$q = v_\perp \cdot i_q^* = v_\perp^+ \cdot i_q^* + v_\perp^- \cdot i_q^* = Q + \tilde{q} \tag{2-39}$$

where $\tilde{p}$ and $\tilde{q}$ are power oscillation at twice the fundamental frequency.

In the BPSC strategy, both the instantaneous active and reactive power will consist of oscillatory term under unbalanced grid, which is different from the previous control strategies.

2.3 Simulation results

In order to validate the aforementioned reviewed control strategies, unbalanced voltage is the simulation is implemented in Matlab/Simulink environment. TABLE 2.1 shows the parameter for the simulation and active power reference is set to be 2.5KW, reactive power is set to be zero.

TABLE 2. 1Simulated System Parameters.

	Symbol	Value
DC link voltage	v_{dc}	700V
Nominal active power	P^*	2.5KW
Nominal reactive power	Q^*	0Var
Grid inductor	L_g	5mH
Grid voltage(phase to phase)	v_g	380V
Inverter Inductor	L_c	2mH

A. IARC Control Strategy

The current waveforms and output active and reactive power for this control strategy are illustrated in Fig.2.2 (a) and (b). As is mentioned, from *t*=0.2s to *t*=0.3s, the IARC strategy is applied, the current waveforms become very distorted (shown

in Fig.2.2 (a)) in order to fulfill the unity power factor control in the situation of unbalanced voltage in the PCC.

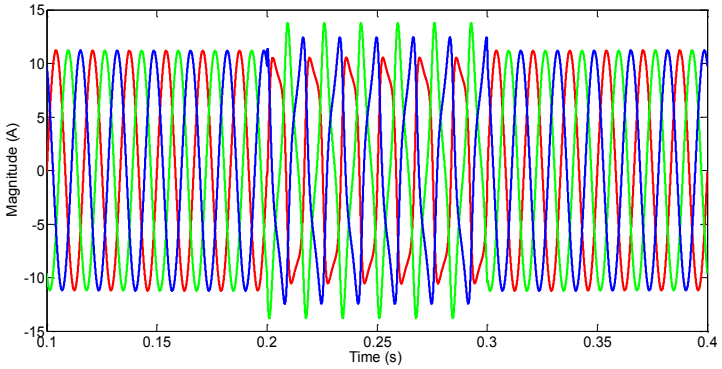

(a)

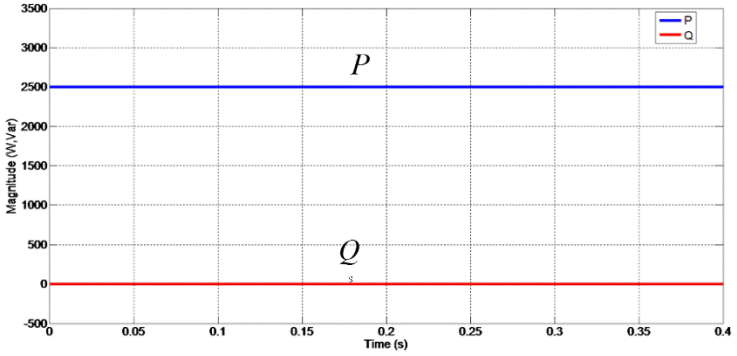

(b)

Fig.2. 2 IARC Strategy (a) grid current and (b) active and reactive powers that delivered to the grid.

B. PNSC Control Strategy

Fig.2.3 (a) and (b) shows the grid currents and active and reactive power that are delivered to the utility grid when PNSC is used (from t=0.2s to t=0.3s). As this control strategy injects negative sequence current in order to cancel the oscillations in active power, in this case, the reference currents consists of a set of unbalanced three phase signals, but without harmonics. Measured current is in accordance with reference current (Fig.2.3a), no oscillations can be observed (Fig.2.3b) in active power waveforms as well.. Large oscillations on the reactive power waveform (Fig.2.3b) could be noticed in this situation due to the interaction between the negative-sequence active current with positive-sequence voltage and positive-sequence active current with negative-sequence voltage.

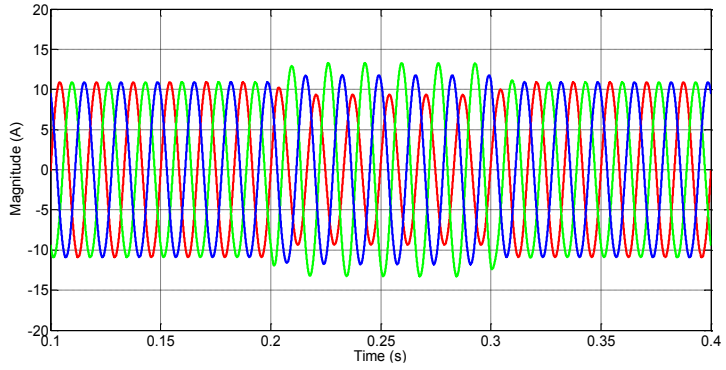

(a)

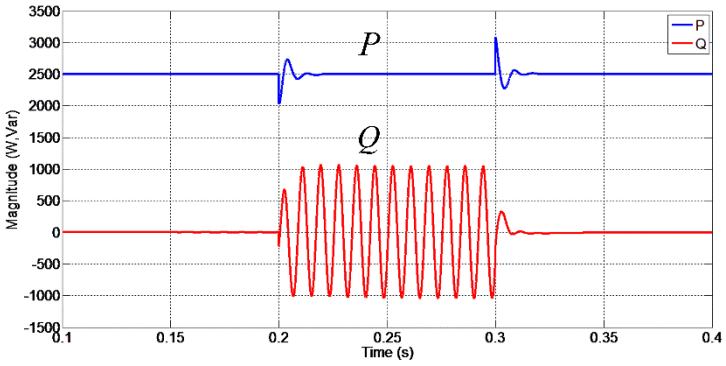

(b)

Fig.2. 3 PNSC Strategy (a) grid current and (b) active and reactive powers delivered to the grid.

C. AARC Control Strategy

From t=0.2s to t=0.3s, the current reference generator implements AARC control strategy. As is seen from Fig.2.4a, the measured grid current is sinusoidal but .unbalanced the reactive power registers no oscillation, but the active power exhibits large oscillations at double the fundamental frequency due to the oscillation in $|V^2|$ (Fig.2.4b).

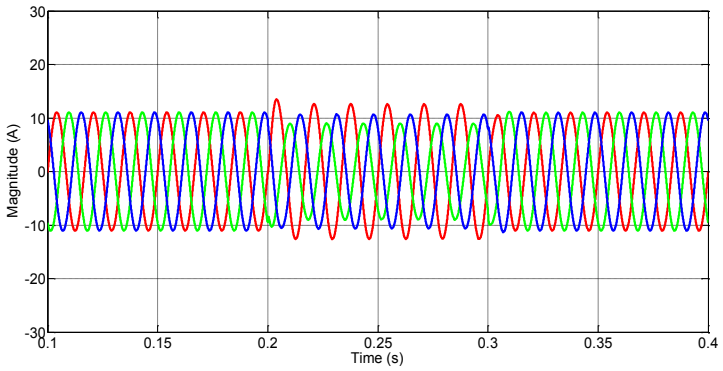

(a)

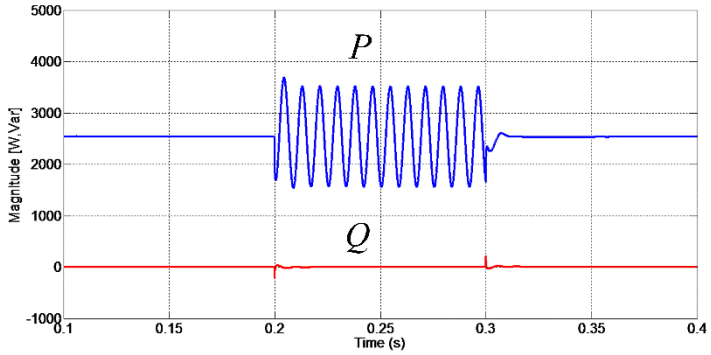

(b)

Fig.2. 4 AARC Strategy (a) grid current and (b) active and reactive powers delivered to the grid.

D. BPSC Control Strategy

Fig.2.5 (a) and (b) shows the current and power waveforms in the case of BPSC control (from t=0.2s to t=0.3s). As only the positive sequence component of the grid voltage is used for calculating the grid current reference, the currents are sinusoidal and balanced (Fig.2.5a). In this case the oscillations are at double the fundamental frequency in both active and reactive powers (Fig.2.5b)

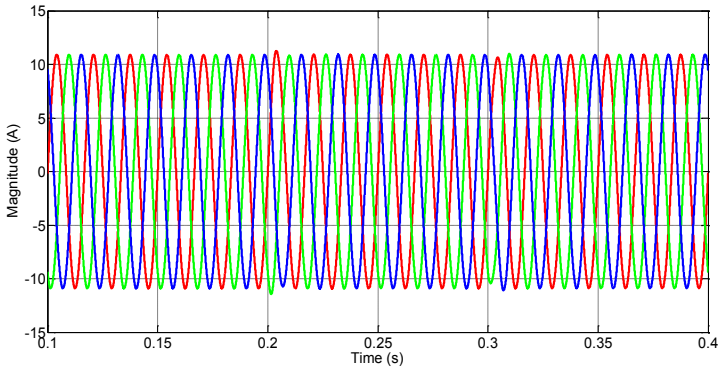

(a)

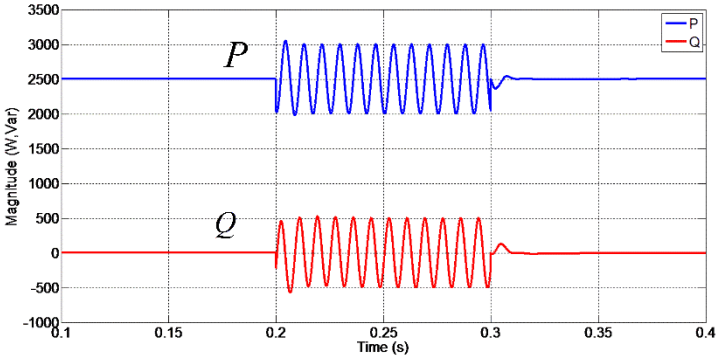

(b)

Fig.2. 5BPSC Strategy (a) grid current and (b) active and reactive powers delivered to the grid.

2.4 Summary

The unbalanced grid voltage may affect the normal operation of DG's power electronic converters. As presented in this chapter, four methods dealing with control of distributed generation system have been reviewed when unbalance voltage happened in the grid. The results shows that the design of flexible active power controller is capable to adapt to unbalance situation in case of grid requirement change. Particularly, it has been proven that it is possible to obtain zero active and reactive power oscillation at the DG output. This is done by injecting

negative current to cancel the power oscillation such as PNSC and AARC. This chapter mainly focus on review and study of DG control scheme under voltage unbalance, some control ideas are adopted in the next chapter when developing DG control strategies for voltage unbalance compensation.

Chapter 3 DG Control Strategies for Voltage Unbalance Compensation

3.1 Introduction

Inverter based DG can provide extra functions, such as unbalanced voltage compensation, harmonic compensation and voltage support beyond power delivery. This chapter proposes to ease grid voltage unbalance with minimization of active power in distributed generation systems. Specifically, the functions to decrease negative sequence voltage and minimize active power at the PCC are realized in the control of distributed generation inverters. The purpose of minimizing active power is to smooth the dc link voltage oscillation, resulting in the benefits of better harmonic suppression and smaller dc link capacitor. To reduce the effects of active power oscillations, two control strategies are proposed for DG to compensate the grid voltage unbalance using instantaneous power theory. In the first method, active power oscillatory cancellation strategy is adopted. In this method, the active power oscillation is controlled to be zero. However, the level of the negative sequence voltage reduction is not controllable. The second control strategy is proposed to alleviate negative sequence voltage and minimize the active power oscillation at PCC by optimizing the phase angle of the DG injected negative sequence current using an on-line Lagrange optimization method. With this method, adjustable level of unbalance compensation can be achieved with minimized active power oscillation. The validity of these two control strategies are verified by simulation results using Matlab/Simulink.

3.2 Principle of Unbalanced Voltage Compensation

Fig.3.1 shows the DG connected to the grid through a voltage source inverter (VSI). The VSI incorporates a two level three phase voltage source converter with L filter. Finally, the DG inverter is connected to the utility at PCC, where unbalanced loads are also connected. It is noted that R_L and L_L are equivalent resistance and inductance of inverter side, and R_g and L_g represent feeder resistance and inductance up to the PCC, respectively.

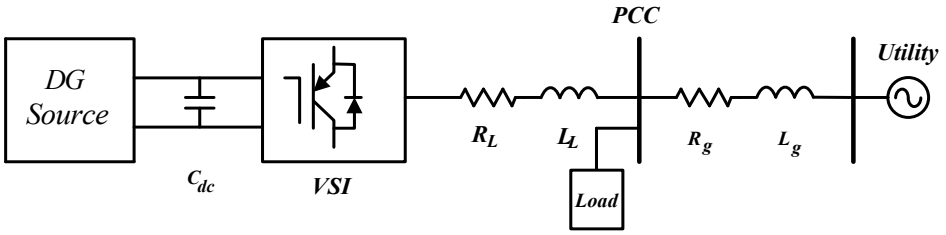

Fig.3. 1: Grid connected DG inverter with unbalanced load.

According to instantaneous power theory that has been stated, power injected into the grid is described as:

$$p = v \cdot i \tag{3-1}$$

where $v = [\, v_a, v_b, v_c], i = [i_a, i_b, i_c]^T$. Considering the sequence component in the voltage and current, (3-1) is described as [40] :

$$p = (v^+ + v^-) \cdot (i^+ + i^-) \tag{3-2}$$

When expanding the equation (3-2), the following equation is derived [40]:

$$p = v^+ \cdot i^+ + v^- \cdot i^- + v^+ \cdot i^- + v^- \cdot i^+ = P + \tilde{p} \tag{3-3}$$

where $P = v^+ \cdot i^+ + v^- \cdot i^-$ and $\tilde{p} = v^+ \cdot i^- + v^- \cdot i^+$, and v^+, v^-, i^+, i^- are positive and negative sequence component of voltage and current vector, P is average value of active power and $\tilde{p}$ is oscillatory term of active power.

Likewise, reactive power at the PCC could be expressed as [41]:

$$q = v_\perp \cdot i \tag{3-4}$$

where $v_\perp$is the 90 degree lagging the measured voltage, and could be referred as:

$$v_{\perp} = \frac{1}{\sqrt{3}} \begin{bmatrix} 0 & 1 & -1 \\ -1 & 0 & 1 \\ 1 & -1 & 0 \end{bmatrix} v \tag{3-5}$$

The expression in equation could be described as sequence component function [41]:

$$q = (v_{\perp}^{+} + v_{\perp}^{-}) \cdot (i^{+} + i^{-}) \tag{3-6}$$

$$q = v_{\perp}^{+} \cdot i^{+} + v_{\perp}^{-} \cdot i^{-} + v_{\perp}^{+} \cdot i^{-} + v_{\perp}^{-} \cdot i^{+} = Q + \tilde{q} \tag{3-7}$$

where $Q = v_{\perp}^{+} \cdot i^{+} + v_{\perp}^{-} \cdot i^{-}$ and $\tilde{q} = v_{\perp}^{+} \cdot i^{-} + v_{\perp}^{-} \cdot i^{+}$. The $Q\ and\ \tilde{q}$ are average and oscillatory values of reactive power, respectively. According to (3-1) and (3-4), current which is in the same direction with voltage will generate active power, meanwhile, current which is aligned with $v_{\perp}$ will give rise to reactive power [41]. Therefore, current reference could be expressed as [40]:

$$\begin{cases} i_p^* = gv \\ i_q^* = bv_{\perp} \end{cases} \tag{3-8}$$

where $g = \frac{P}{|v|^2}, b = \frac{Q}{|v|^2}$. Total reference current could be obtained as follows:

$$i^* = i_p^* + i_q^* \tag{3-9}$$

Expanding (3-9), instantaneous conductance g could be separated into positive sequence and negative sequence: g^+ and g^-. So, reference current generated by active power could be described as [42]:

$$i_p^* = g^+ v^+ + g^- v^- \tag{3-10}$$

where $g^+ = \frac{P}{|v^+|^2}, g^- = \frac{P}{|v^-|^2}$. If it needs to inject both positive and negative sequence current into the grid, it is necessary to regulate both of them to keep reference active power constant. Based on this point, we could define a parameter k_1 to regulate the proportion of each sequence current delivered into the grid [42]:

$$i_p^* = k_1 \frac{P}{|v^+|^2} v^+ + (1 - k_1) \frac{P}{|v^-|^2} v^- \tag{3-11}$$

Meanwhile, another parameter could be set as k_2 to regulate positive and negative sequence of reactive power reference current. The expression could be referred as [42]:

$$i_q^* = k_2 \frac{Q}{|v^+|^2} v_\perp^+ + (1 - k_2) \frac{Q}{|v^-|^2} v_\perp^- \tag{3-12}$$

Finally, considering (3-9), the total reference current could be expressed as [42]:

$$i^* = P \left(\frac{k_1}{|v^+|^2} v^+ + \frac{(1-k_1)}{|v^-|^2} v^- \right) + Q \left(\frac{k_2}{|v^+|^2} v_\perp^+ + \frac{(1-k_2)}{|v^-|^2} v_\perp^- \right) \tag{3-13}$$

Therefore, instantaneous active power at PCC is calculated as:

$$p = (v^+ + v^-) \cdot i^* = P + \tilde{p} \tag{3-14}$$

In (3-14), P and $\tilde{p}$ can be defined as:

$$P = \frac{Pk_1}{|v^+|^2} \cdot v^+ \cdot v^+ + \frac{P(1-k_1)}{|v^-|^2} \cdot v^- \cdot v^- \tag{3-15}$$

$$\tilde{p} = \left(\frac{Pk_1}{|v^+|^2} + \frac{P(1-k_1)}{|v^-|^2} \right) v^+ \cdot v^- + \left(\frac{Qk_2}{|v^+|^2} - \frac{Q(1-k_2)}{|v^-|^2} \right) \cdot v_\perp^+ \cdot v^- \tag{3-16}$$

Considering (3-16), it is observed that active power oscillation problems will occur at PCC when DG sends both active power and reactive power to the grid under voltage unbalance conditions. However, properly designed k_1 and k_2 could possibly alleviate active power oscillation while compensating the unbalance voltage.

3.3 Negative Sequence equivalent circuit analysis

In grid-connected DG systems, the injection of negative sequence active and reactive powers can help voltage unbalance compensation and reduce active power oscillation. The negative sequence equivalent circuit of grid-connected DG is shown in Fig.3. 2 In this figure, Z_R indicates equivalent impedance when active power is injected into the grid ($Z_R = \frac{V_{PCC}^-}{i_P^-}$), and Z_L indicates equivalent impedance when reactive power is injected into the grid ($Z_L = \frac{V_{PCC}^-}{i_q^-}$). Moreover, the unbalanced load connected to PCC behaves as a constant current source I_{load}^-.

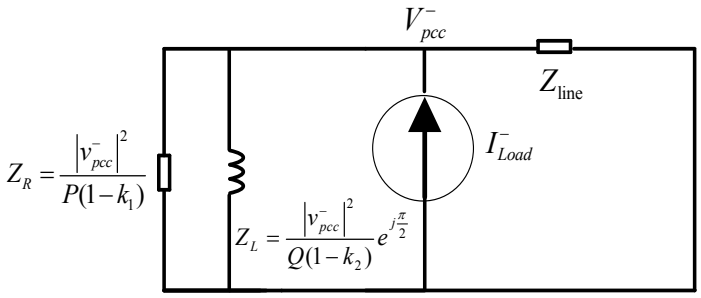

Fig.3. 2 Negative sequence equivalent circuit.

In this analysis, two scenarios are explained as following:

3.3.1 Without injection of negative sequence active and reactive powers

This is the case when $k_1 = 1$ and $k_2 = 1$, where just positive sequences of active and reactive powers are injected to the grid. Considering Fig.3. 2, both Z_R and Z_L are open circuit, and V_{PCC}^{-} can be expressed as:

$$|V_{PCC}^{-}| = |I_{load}^{-}| \times |Z_{line}| \tag{3-17}$$

3.3.2 Injection of negative sequence active and reactive Powers

In the case that both active and reactive power's negative sequences are injected to the grid, k_1 and k_2 should be $k_1 \neq 1$ and $k_2 \neq 1$. Considering Fig.3. 2, V_{PCC}^{-} can be expressed as:

$$|V_{PCC}^{-}| = |I_{load}^{-}| \times |Z_{line} \parallel Z_R \parallel Z_L| \tag{3-18}$$

For negative sequence voltage reduction at PCC, $|V_{PCC}^{-}|$ in (3-19) should be smaller than $|V_{PCC}^{-}|$ in (3-18). Considering the same load (the same current source I_{load}^{-}), $|Z_{line} \parallel Z_R \parallel Z_L|$ should be smaller than $|Z_{line}|$. Therefore, the chosen values of k_1 and k_2 should satisfy the following expression:

$$\left| \frac{1}{\frac{1}{Z_R}+\frac{1}{Z_L}+\frac{1}{Z_{Line}}} \right| = \left| \frac{1}{\frac{1}{\frac{|V_{PCC}^{-}|^2}{P(1-k_1)}}+\frac{1}{\frac{|V_{PCC}^{-}|^2}{Q(1-k_2)}e^{j\frac{\pi}{2}}}+\frac{1}{Z_{Line}}} \right| < |Z_{line}| \tag{3-19}$$

From Fig.3.2, in the case that $k_1 \neq 1$ and $k_2 = 1$, just the negative sequence of active power is injected to the grid (Z_L is open circuit in Fig.3.2), and $\frac{1}{Z_L}$ become

zero in . Moreover, $k_1 = 1$ and $k_2 \neq 1$ lead to the injection of negative sequence reactive power to the grid (Z_R is open circuit in Fig.3.2), and $\frac{1}{Z_R}$ become zero in (3-19).

3.4 Control Strategies for Voltage Unbalance Compensation

In this section, the proposed control strategies will be explained in details. There will be two unbalanced voltage compensation strategies in the following including strategy for cancellation of active power oscillation with uncontrollability of unbalanced voltage compensation and strategy for minimizing active power oscillation with adjustable level of unbalanced voltage compensation.

3.4.1 Strategy for cancellation of active power oscillation

This strategy is designed for completely eliminating active power oscillation. In this control strategy, cancelling the active power oscillation leads to unbalance voltage reduction, too. From (3-16), it could be observed that in order to meet the requirement of power oscillation to be zero, following (3-20)-(3-21) equations need to be satisfied.

$$\frac{Pk_1}{|v^+|^2} + \frac{P(1-k_1)}{|v^-|^2} = 0 \Rightarrow k_1 = \frac{|v^+|^2}{|v^+|^2 - |v^-|^2} \tag{3-20}$$

$$\frac{Qk_2}{|v^+|^2} - \frac{Q(1-k_2)}{|v^-|^2} = 0 \Rightarrow k_2 = \frac{|v^+|^2}{|v^+|^2 + |v^-|^2} \tag{3-21}$$

This method is similar with PNSC method in the previous chapter. Details for this control strategy are shown in Fig.3.3. First, unbalanced voltage is detected and separated into positive and negative sequence using Frequency-Locked Loop(FLL) [43]. Then, k_1 and k_2 are calculated according to equation (3-20) and (3-21). Using calculated k_1 and k_2 with the supplied average active power P and average reactive power Q, the reference currents are generated on account of equation (3-13).

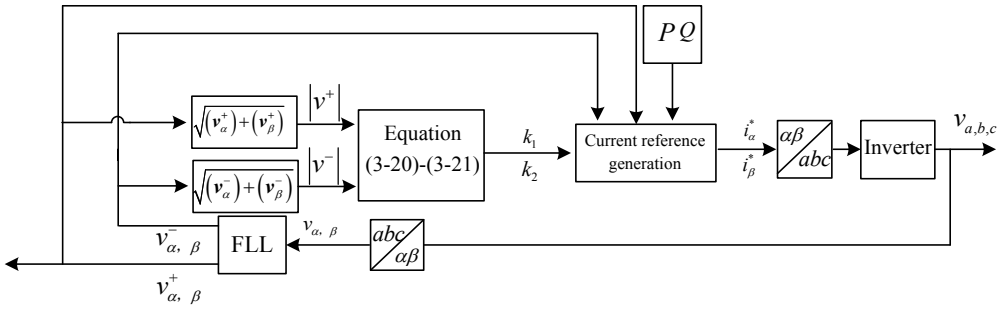

Fig.3. 3 DG control scheme in active power oscillation cancellation strategy.

Although this method could fully cancel out the active power oscillation, its capability of reducing negative sequence voltage is limited. In order to largely reduce the negative sequence voltage at PCC, a new optimized method is proposed to overcome the disadvantage of the first method. Detailed description of this method is in the next section.

3.4.2 Minimization of active power oscillation with adjustable unbalance compensation

This method is proposed for adjustable unbalance voltage compensation (according to DG available power rating) while at the same time minimizing the active power oscillation (instead of completely cancel it). In this method, the negative sequence virtual impedance presented by DG (see Fig.3. 2) can be controlled to be much smaller than the grid impedance, and therefore the unbalance current from the load flows to the DG side, leading to an improved PCC voltage. Based on this idea, we define $\left|i_{ref}^{-}\right|$ as the magnitude of desired negative sequence current generated by DG in(3-22).

$$\left|i_{ref}^{-}\right| = \sqrt{\left(\frac{P(1-k_1)}{|v^{-}|}\right)^2 + \left(\frac{Q(1-k_2)}{|v^{-}|}\right)^2} \tag{3-22}$$

This desired current generated by DG could be controlled as $i_{ref}^{-} = \frac{V^{-}}{|Z_{DG}|}$. It is clear to see that k_1 and k_2 are in the following boundary:

$$1 - \frac{|v^-||i_{ref}|}{P} \leq k_1 \leq 1 + \frac{|v^-||i_{ref}|}{P} \quad (3\text{-}23)$$

$$1 - \frac{|v^-||i_{ref}|}{Q} \leq k_2 \leq 1 + \frac{|v^-||i_{ref}|}{Q} \quad (3\text{-}24)$$

Meanwhile, based on (3-16), active power oscillation at PCC could be described as:

$$\tilde{p} = \left(\frac{Pk_1}{|v^+|^2} + \frac{P(1-k_1)}{|v^-|^2}\right)|v^+||v^-|cos2wt + \left(\frac{Qk_2}{|v^+|^2} - \frac{Q(1-k_2)}{|v^-|^2}\right)|v^+||v^-|sin2wt \quad (3\text{-}25)$$

In order to minimize active power oscillation represented in(3-25), following objective function can be considered:

Objective function:

$$\left[\left(\frac{Pk_1}{|v^+|^2} + \frac{P(1-k_1)}{|v^-|^2}\right)|v^+||v^-|\right]^2 + \left[\left(\frac{Qk_2}{|v^+|^2} - \frac{Q(1-k_2)}{|v^-|^2}\right)|v^+||v^-|\right]^2 \quad (3\text{-}26)$$

This equation should be minimized considering (3-22) as a constraint (negative sequence of current constraint). If we assume that:

$$k_1 - 1 = l_1 \quad (3\text{-}27)$$

$$k_2 - 1 = l_2 \quad (3\text{-}28)$$

The objective function and constraint function could be expressed as following.

$$\text{Objective function:} \qquad J = A^2 l_1^2 + B^2 l_2^2 + C l_1 + E l_2 + F \quad (3\text{-}29)$$

Constraint is expressed as:

$$P^2 l_1^2 + Q l_2^2 = D^2 \quad (3\text{-}30)$$

where $A, B, C, D, E,$ and F are defined as:

$A = \frac{P(|v^+|^2 - |v^-|^2)}{|v^+||v^-|}$, $B = \frac{Q(|v^+|^2 - |v^-|^2)}{|v^+||v^-|}$ $C = \frac{2P^2|v^-|^2(|v^+|^2 - |v^-|^2)}{|v^+|^2|v^-|^2} D = |v^-|i_{ref},$ $E = \frac{-2Q^2|v^-|^2\left(|v^+|^2 + |v^-|^2\right)}{|v^+|^2|v^-|^2}$, $F = \frac{|v^-|^4(P^2+Q^2)}{|v^+|^2|v^-|^2}$.

Various optimization methods can be used to minimize the objective function considering its constraints. In this paper, Lagrange method is used for minimization purpose as following [44]:

$$H = J + \lambda(P^2 l_1^2 + Q l_2^2 - D^2) \tag{3-31}$$

The conditional extreme for the equation is as following:

$$\frac{\partial H}{\partial l_1} = 0 \Rightarrow l_1 = \frac{-C}{2A^2 + 2\lambda P^2} \tag{3-32}$$

$$\frac{\partial H}{\partial l_2} = 0 \Rightarrow l_2 = \frac{-E}{2B^2 + 2\lambda Q^2} \tag{3-33}$$

$$\frac{\partial H}{\partial \lambda} = 0 \Rightarrow P^2 l_1^2 + Q^2 l_1^2 - D^2 = 0 \tag{3-34}$$

From (3-32)-(3-34), the value of l_1, l_2 and λ are calculated, then k_1 and k_2 are calculated from (3-27) and (3-28).

Fig.3.4 shows the block diagram of the control strategy with Lagrange optimization scheme. Voltage at PCC is first detected and separated into positive sequence and negative sequence using FLL [43]. Magnitude of negative sequence voltage is calculated, and then divided by virtual impedance $|Z|$ to generate a certain negative sequence current value i_{ref}. Then k_1 and k_2 are calculated using optimized method. Finally, reference current could be derived according to equation (3-13).

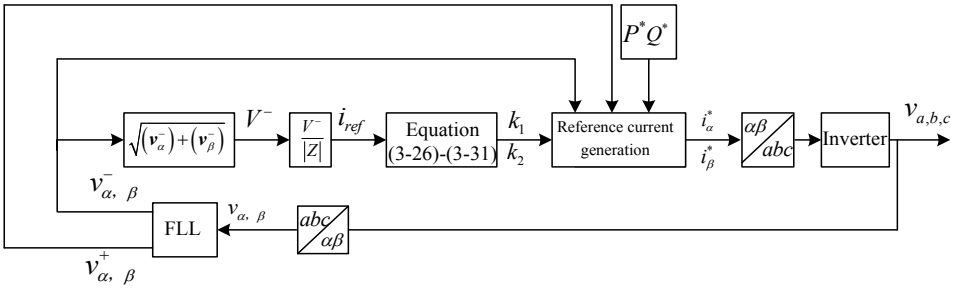

Fig.3. 4DG Control scheme in reduction of voltage unbalance and minimization of active power oscillation strategy

3.4.3 Current control scheme

The block diagram of current control scheme is shown in Fig.3.5. Based on the current command i^*, the measured current i, and the voltage at PCC, current regulator produces voltage reference for the interfacing VSI. In this control system, the transfer function of proportional plus resonant controller is defined as:

$$H(s) = k_p + \frac{2K_i\xi w_f s}{s^2+2\xi w_f s+w_f^2} \quad (3\text{-}35)$$

where k_p represent the proportional gain, K_i is the integral gain, w_f is the fundamental frequency. In (3-35), the ξ is the damping ratio to generate a narrow gain peak at the fundamental frequency of current. In this control scheme, feed-forward control is used to decouple voltage disturbance from the current control loop.

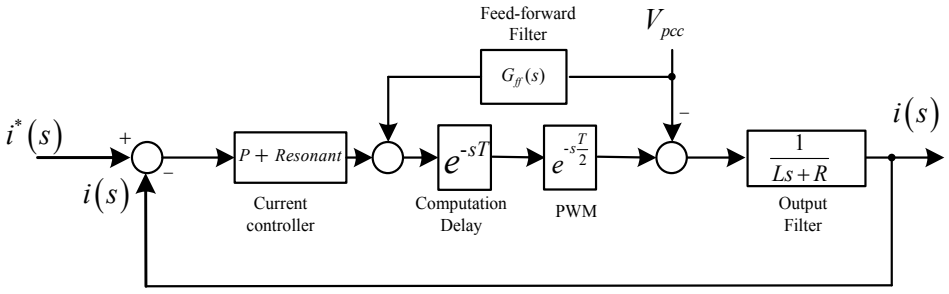

Fig.3. 5Current control loop diagram.

3.5 DC link voltage control under unbalanced voltage

As the active power oscillation can have great influence on the DC link voltage, control of DC link needs to be investigated. When PCC is subject to unbalanced load or asymmetrical fault, DC link voltage will suffer a sinusoidal voltage oscillation with frequency of $2w_0$, Proper operation of VSC requires its dc-side voltage is tightly controlled during steady-state and dynamic periods. This section describes an accurate non-linear model for dc-side voltage control, considering the ac-side inductor. The non-linear model is then linearized at operating point to assist the design of DC link voltage controller.

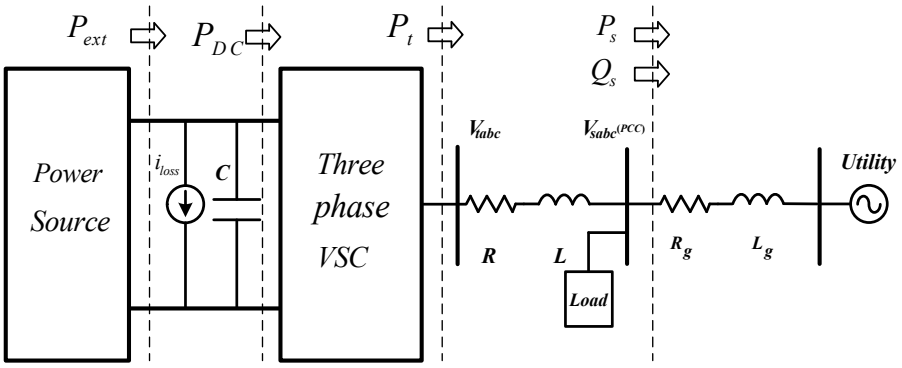

Fig.3. 6 Power delivery through DC link

3.5.1 Mathematical model.

Fig.3.6 shows a schematic diagram of power flow through DC link. The power source typically represents PV array, variable speed wind turbine, or fuel-cell unit [36]. Here we consider it as a black box and represent as P_{ext}. In this figure, the power balance is formulated as [45]:

$$\left(\frac{C}{2}\right)\frac{dV_{dc}^2}{dt} = P_{ext} - P_t - P_{loss} \tag{3-36}$$

where $P_{loss} = V_{DC} i_{loss}$, P_t is the VSC AC side terminal power. In this equation, it could be observed that V_{DC}^2 is the state variable and output, P_t is the control input, and P_{ext} and P_{loss} is the disturbance input.

Since VSC system of Fig.3.6 enables to control DG output power P_s and Q_s, so P_t is expressed in terms of P_s and Q_s

$$L\frac{di}{dt} = -Ri + V_t - V_{pcc} \tag{3-37}$$

By multiplying both sides of (3-37) with (3/2) i, we could get

$$P_t = P_s + \frac{3}{2}Ri^2 + \frac{3}{4}L\frac{di^2}{dt} \tag{3-38}$$

Based on the following equation

$$P_S + jQ_S = \frac{3}{2}V_{pcc} \times i^* \tag{3-39}$$

We could deduce

$$P_s^2 + Q_s^2 = \frac{9}{4}V_{pcc}^2 \times i^2 \tag{3-40}$$

Substitute for i^2 from (3-40) in (3-38)and assume V_{pcc} is constant, we obtain:

$$P_t = P_s + \left(\frac{2L}{3V_{pcc}^2}\right) P_s \frac{dP_s}{dt} + \left(\frac{2L}{3V_{pcc}^2}\right) Q_s \frac{dQ_s}{dt} \tag{3-41}$$

Substituting for P_t from (3-41) in (3-36), we have

$$\left(\frac{c}{2}\right)\frac{dV_{dc}^2}{dt} = P_{ext} - P_s - \left(\frac{2L}{3V_{pcc}^2}\right) P_s \frac{dP_s}{dt} - \left(\frac{2L}{3V_{pcc}^2}\right) Q_s \frac{dQ_s}{dt} \tag{3-42}$$

Due to the presence of terms $P_s \frac{dP_s}{dt}$ and $Q_s \frac{dQ_s}{dt}$, the control plant is non-linear, so first, we need to linearize about a steady-state operating point, which is computed by replacing all the derivatives by zero.

$$P_{s0} = P_{ext0} - P_{loss} = P_{ext0}$$

After linearization

$$\left(\frac{c}{2}\right)\frac{dV_{dc}^2}{dt} = \frac{2}{c}\tilde{P}_{ext} - \frac{2}{c}\left[\tilde{P}_s + \left(\frac{2LP_{s0}}{3\tilde{V}_S^2}\right)\right]\frac{d\tilde{P}_s}{dt} + \frac{2}{c}\left(\frac{2LQ_{s0}}{3\tilde{V}_S^2}\right)\frac{d\tilde{Q}_s}{dt} \tag{3-43}$$

where the symbol $\sim$ denotes small perturbations.

So, the transfer function from $\tilde{P}_s(s)$ to $\tilde{V}_{DC}^2$ is described as:

$$G_v = \frac{\tilde{V}_{DC}^2}{\tilde{P}_s(s)} = -\left(\frac{2}{C}\right)\frac{\tau s+1}{s} \tag{3-44}$$

where $\tau = \frac{2LP_{ext0}}{3\widehat{V_S^2}}$

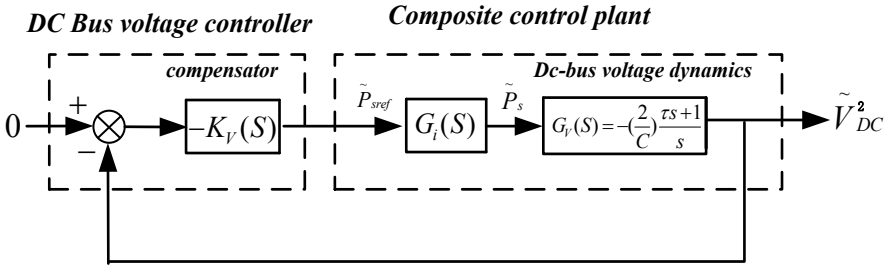

Fig.3. 7Control block diagram of DC bus voltage regulator

3.5.2Controller design

Fig.3.7 shows the control block diagram of DC-bus voltage control loop based on the model of plant. Under unbalanced load condition, there exists double frequency ripple component of V_{dc}^2. Therefore, $K_V(s)$ must exhibit a low gain at $2w_0$ to attenuate the ripple component of V_{dc}^2. Meanwhile to achieve zero steady-

state error, $K_V(s)$ must include at least one pole at s=0. Due to the existing pole in the model $G_V(s)$, the open loop transfer function consists of double pole at origin. Hence the design is chosen by using symmetrical optimum design criteria. The advantage for this method is to maximize the phase margin at cross-over frequency. So the system can withstand more delays.

First assume the PI compensator is

$$K_V(s) = k\frac{s+z}{s} \tag{3-45}$$

Then the loop gain is:

$$l(\mathrm{s}) = \frac{k}{\tau_i C}\left(\frac{s+z}{s+\tau_i^{-1}}\right)\frac{\tau s+1}{s^2} \tag{3-46}$$

At low frequency $\angle l(jw) = -180$ due to the double pole at s=0, if $z < \tau_i^{-1}$, $\angle l(jw)$ first increase until it reach a maximum δ_m at a certain frequency w_m, then for $w > w_m$, $\angle l(jw)$ drops , δ_m and w_m are calculated by

$$\delta_m = sin^{-1}\left(\frac{1-\tau_i z}{1+\tau_i z}\right) \tag{3-47}$$

And $w_m = \sqrt{z\tau_i^{-1}}$, so crossover frequency w_c is chosen as w_m

Here we choose phase margin at 53, and $\tau_i = 2 \times 10^{-3}$, so, according to the symmetrical optimum design criteria and notch filter addition. We have the controller:

$$K_V(s) = 0.4\frac{s+50}{s}\cdot \tag{3- 48}$$

Fig.3. 8 shows the loop gain magnitude and phase plot of the load voltage regulator using the compensator. From the figure, it can be observed that the phase margin is 53 and $w_c = 256rad/s$ at the cross over frequency, effectiveness of this controller will be simulated in the Section 3.7.

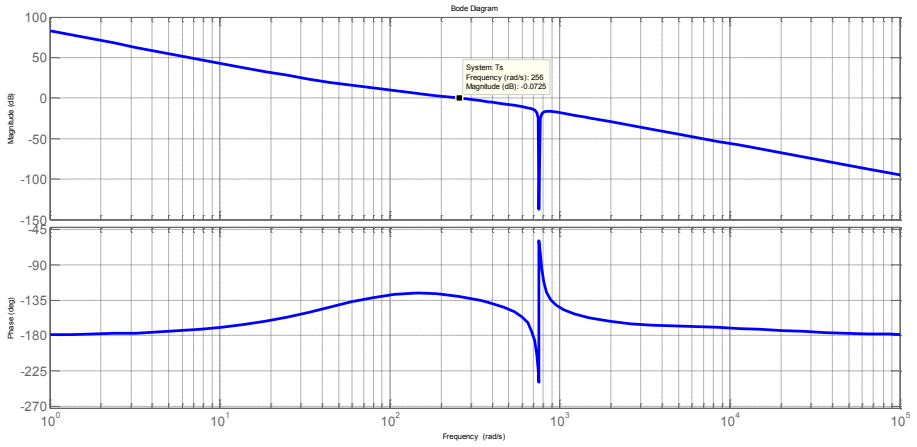

Fig.3. 8 Open loop frequency response

3.6 Detection of positive and negative sequence components

3.6.1 Principle of separation for unbalanced voltage

Precise detection of unbalanced grid voltage is crucial in order to fully control the power electronic devices that deliver power from DG into grid. Various types of unbalanced voltage detection methods have been presented [46], such as Fourier-transformation-based detection [47], the delayed signal cancellation-based detection [48], and second-order generalized integrator (SOGI) [43], etc.

In this work, a detection method by means of a positive-negative sequence voltage detector based on second-order generalized integrator is adopted and briefly reviewed [49].

The core part of the detector-SOGI diagram is shown in Fig.3.9 and its transfer function is

$$S(s) = \frac{y}{x}(s) = \frac{w_0 s}{s^2 + w_0^2} \tag{3-49}$$

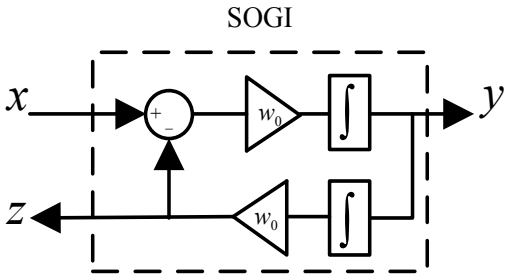

Fig.3. 9 Structure of SOGI [49]

where w_0 is the SOGI resonance frequency. If $x = Xsin(wt + \theta)$ and SOGI is considered as an ideal integrator when $w = w_0$, the closed loop diagram that is shown in Figure 3.10 gives rise to a second band pass filter(BPF) whose transfer function is (3-50) and (3-51). Both (3-50) and (3-51) shows the SOGI-QSG scheme transfer function.

$$D(s) = \frac{v'}{v}(s) = \frac{kw'}{s^2+kw's+w'^2} \tag{3-50}$$

$$Q(s) = \frac{qv'}{v}(s) = \frac{kw'}{s^2+kw's+w'^2} \tag{3-51}$$

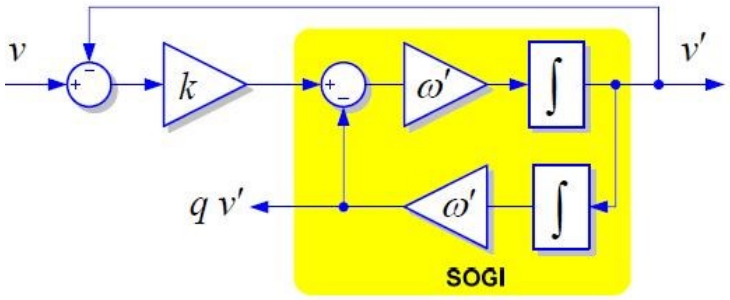

Fig.3. 10structure of SOGI and a band pass filter based on SOGI implementation [49]

The damping factor is related with parameter of k, the characteristic of SOGI in Fig 3.11and Fig.3.12 is suitable for separation of unbalanced voltage

First, if w_0 and k are properly chosen, v_a' will be almost sinusoidal and will match the fundamental component of v_a. Second, signal qv_a' is in quadrature of v_a, which is quite useful for detecting symmetrical voltage component in three phase system. Finally, the SOGI resonance frequency can be adjusted through phase-lock loop, making the system adaptive.

As is shown in Fig.3.11, different value of k will have great influence on the filtering frequency. With a lower value of k, the filtering is more tight around the resonant frequency, however, the system becomes less stable. Meanwhile, a high value of k allows other frequencies to pass through the filter. Therefore, there is a tradeoff for the proper parameter of k selection.

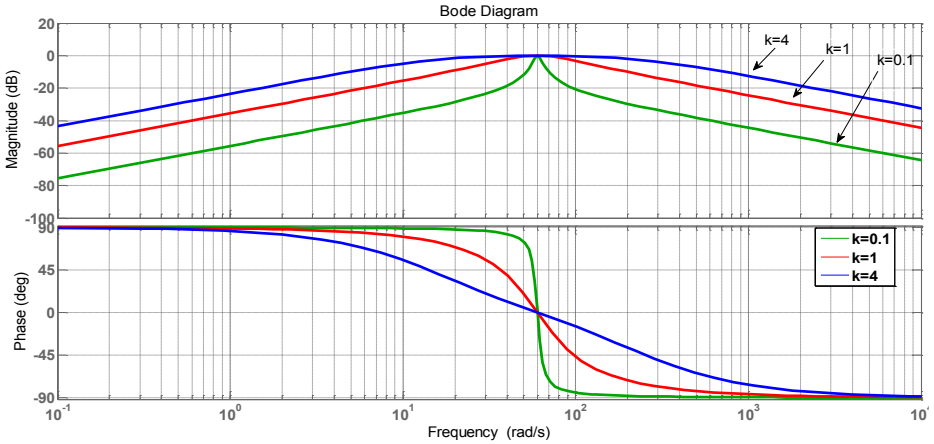

Fig.3. 11Bode plot of SOGI-BPF for different values of gain k

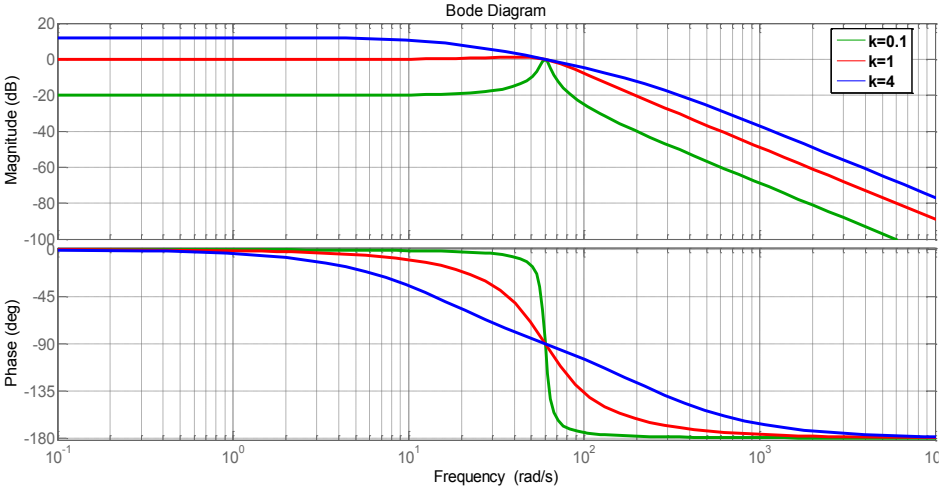

Fig.3. 12Bode plot of Q(s)

The instantaneous positive and negative sequence component is expressed as:

$$\mathrm{v}_{abc}^{+} = [v_a^{+}, v_b^{+}, v_c^{+}]^T = [T_+]\mathrm{v}_{abc} \tag{3-52}$$

$$\mathrm{v}_{abc}^{-} = [v_a^{-}, v_b^{-}, v_c^{-}]^T = [T_-]\mathrm{v}_{abc} \tag{3-53}$$

where $[T_+]$ and $[T_-]$ are defined as:

$$[T_+] = \frac{1}{3}\begin{bmatrix} 1 & a & a^2 \\ a^2 & 1 & a \\ a & a^2 & 1 \end{bmatrix} \tag{3-54}$$

$$[T_-] = \frac{1}{3}\begin{bmatrix} 1 & a^2 & a \\ a & 1 & a^2 \\ a^2 & a & 1 \end{bmatrix} \tag{3-55}$$

with $a = e^{j\frac{2\pi}{3}}$

Meanwhile, after Clark transformation being applied, voltage vector is transformed from abc to $\alpha\beta$ reference frame as follows:

$$\mathrm{v}_{\alpha\beta} = [v_\alpha, v_\beta] = [T_{\alpha\beta}]\mathrm{v}_{abc} \tag{3-56}$$

where $[T_{\alpha\beta}] = \sqrt{\frac{2}{3}}\begin{bmatrix} 1 & -\frac{1}{2} & -\frac{1}{2} \\ 0 & \frac{\sqrt{3}}{2} & -\frac{\sqrt{3}}{2} \end{bmatrix}$

Therefore, the instantaneous positive and negative sequence component on $\alpha\beta$ frame is expressed as:

$$\mathrm{v}^+_{\alpha\beta} = [T_{\alpha\beta}]\mathrm{v}^+_{abc} = [T_{\alpha\beta}][T_+][T_{\alpha\beta}]^T\mathrm{v}_{\alpha\beta} = \frac{1}{2}\begin{bmatrix} 1 & -q \\ q & 1 \end{bmatrix}\mathrm{v}_{\alpha\beta} \tag{3-57}$$

$$\mathrm{v}^-_{\alpha\beta} = [T_{\alpha\beta}]\mathrm{v}^-_{abc} = [T_{\alpha\beta}][T_-][T_{\alpha\beta}]^T\mathrm{v}_{\alpha\beta} = \frac{1}{2}\begin{bmatrix} 1 & q \\ -q & 1 \end{bmatrix}\mathrm{v}_{\alpha\beta} \tag{3-58}$$

with $q = e^{-j\frac{\pi}{2}}$, q is a phase shift operator, which is quadrature-phase waveform of original waveform.

Hence, the phase locked loop system is present in Fig.3.13 for detection of positive and negative sequence on $\alpha\beta$ frame, and the SOGI component is to generate in-phase and quadrature-phase waveform of $\mathrm{v}_{\alpha\beta}$.

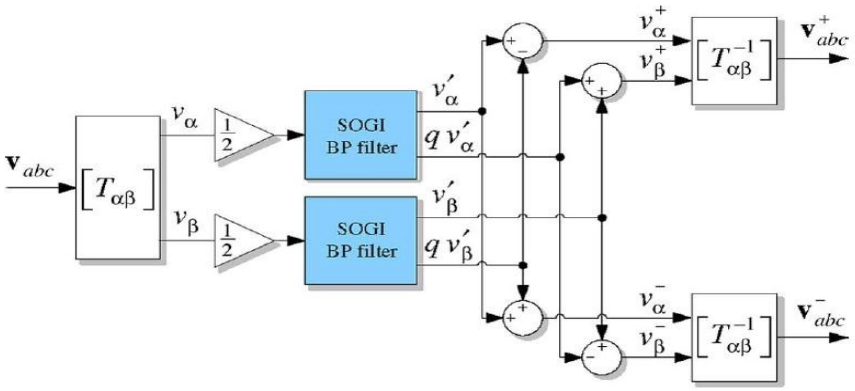

Fig.3. 13 Structure for extracting the positive and negative sequences of the grid voltages based on SOGI-BPF [49].

3.7 Simulation Results

In order to verify the proposed control strategies, two sets of simulation has been carried out in Matlab/Simulink. In the first part, cancellation of active power oscillation control strategy is investigated. In the second part, control strategy for adjustable negative sequence of voltage reduction is evaluated. In following, these two simulation parts are explained in details.

3.7.1 Test 1: Cancellation of active power oscillation

In this part of simulation, single load with 18Ω resistance is connected to the grid at PCC, and $20000W$ average active power and $5000Var$ average reactive power are injected into the grid. The control scheme of active power oscillation is adopted in this simulation. TABLE 3.1 shows the system parameters simulated in this part, and TABLE3.2 depicts the control system parameters. The results are shown from Fig.3.14 to Fig.3.21.

At the beginning of simulation ($t = 0s$), $k_1 = 1$ and $k_2 = 1$ (Figs.3.14 and 3.15), the negative sequence of voltage of PCC is 9.8V (Fig.3.19), and active power oscillation is around 800W (Fig.3.16). In this state, all the negative sequence current

(Fig. 3.17) generated by single load goes through line impedance and the DG current negative sequence is equal to zero (Fig.3.18). At $t = 0.2s$, the active power oscillation cancellation method is applied, which forces active power oscillation to be zero (Fig.3.16). The values of k_1 and k_2 resulted from this method is shown in Fig.3.14 and 3.15. Considering this figures, k_1 and k_2 are not equal to 1 as expected (Eq. (3−17) and (3-18)). Since in this method DG injects the negative sequence of current to the load (Figs.3.17, and3.18), PCC voltage negative sequence is decreased (although the amount of reduction is not very high; Fig.3.19). During the simulation, the positive sequence of PCC voltage (Fig.3.20) remains constant as expected. Meanwhile, from Fig.3. 21 it can be observed that before 0.2s DC link voltage oscillation is around 1.1V and is free of oscillation after the control strategy is implemented.

TABLE 3. 1: System parameters in test 1.

	Symbol	Value
DC link voltage	v_{dc}	800V
Inverter inductor	L	2mH
Inverter inductor resistance	R	1mΩ
Grid inductor	L_g	2mH
Grid inductor resistance	R_g	1mΩ
Single load	R_s	18Ω
Grid voltage	v_g	230V
Average active power	P	20000W
Average reactive power	Q	5000Var

TABLE 3. 2: Control system parameters.

	Symbol	Value
Proportional gain	k_p	2
Resonant gain	k_r	5
Damping factor	ξ	0.1
Fundamental frequency	w_f	60Hz

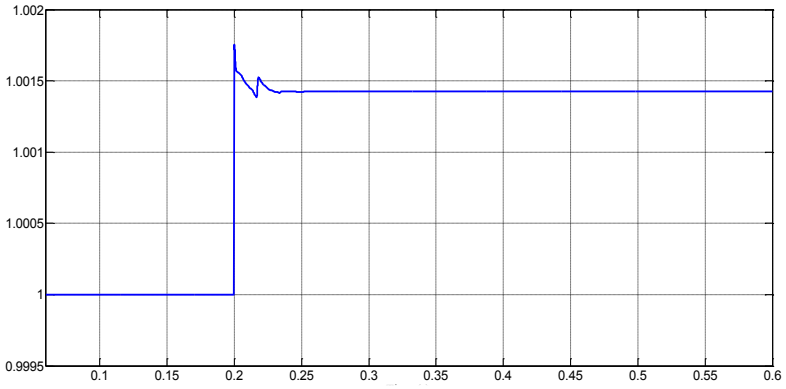

Fig.3. 14 Parameter of $k1$ in test 1

(X-axis: time (s), Y-axis: value of $k1$)

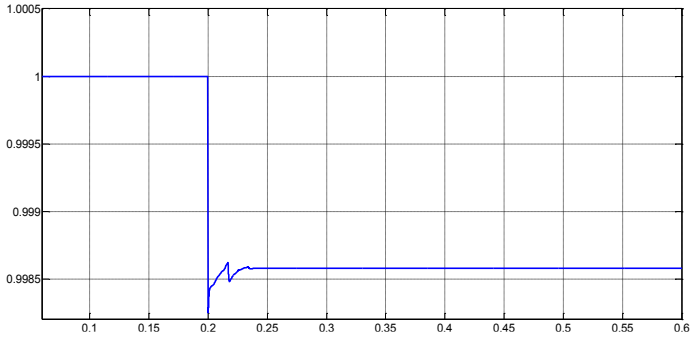

Fig.3. 15 Parameter of $k2$ in test 1.

(X-axis: time (s), Y-axis: value of $k2$)

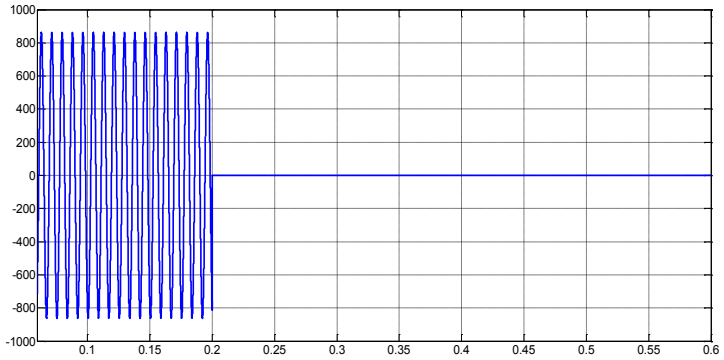

Fig.3. 16 Active power oscillation in test 1.

(X-axis: time (s), Y-axis: active power oscillation(W))

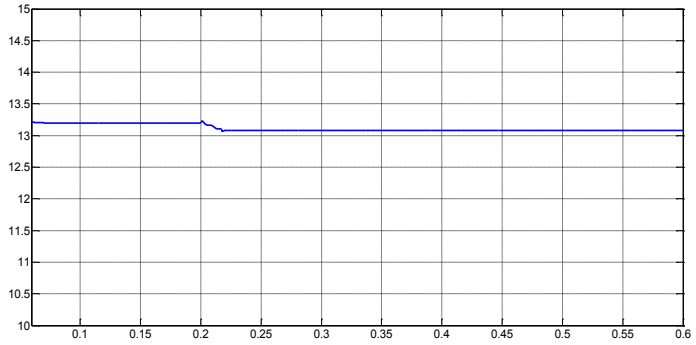

Fig.3. 17 Negative sequence of current going through single load in test 1.

(X-axis: time (s), Y-axis: negative sequence current of sing load (A))

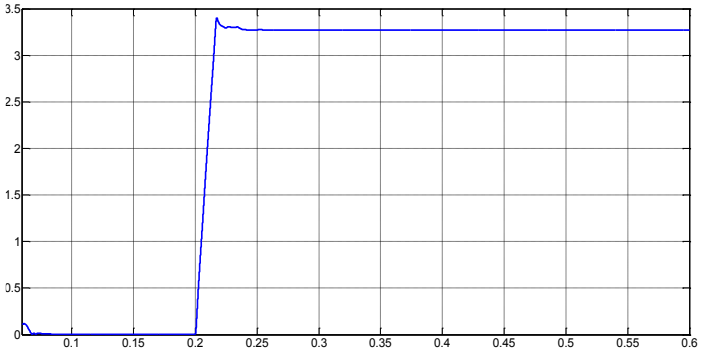

Fig.3. 18 Generated negative sequence of DG current in test 1.

(X-axis: time (s), Y-axis: negative sequence current of DG (A))

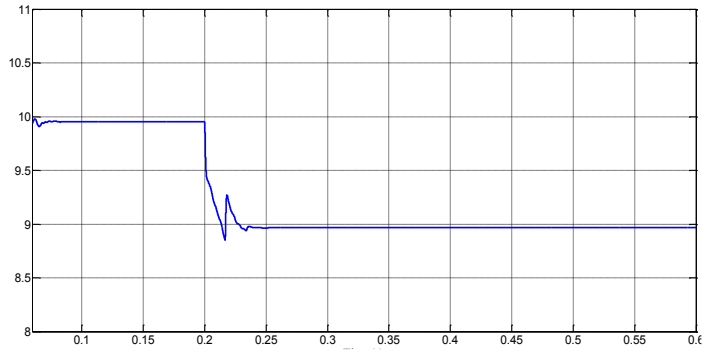

Fig.3. 19 Negative sequence of voltage at PCC in test 1.

(X-axis: time (s), Y-axis: negative sequence voltage at PCC (V))

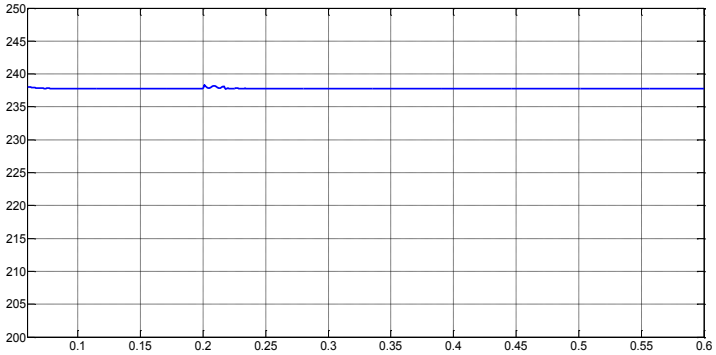

Fig.3. 20 Positive sequence of voltage at PCC in test 1.

(X-axis: time (s), Y-axis: positive sequence of voltage (V))

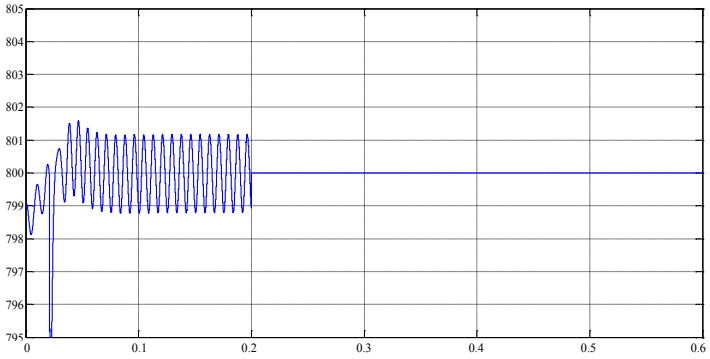

Fig.3. 21 DC link voltage in test 1

(X-axis: time (s), Y-axis: DC link voltage oscillation (V))

3.7.2 Test 2: Negative sequence voltage reduction

In this part of simulation again, the adjustable level of unbalanced compensation

with minimization of active power oscillation is implemented. Single load with 18Ω resistance is connected to the grid at PCC, and 20000W average active power and 5000Var average reactive power are injected into the grid for DG. System parameter is the same with the first test (TABLE3.1), DC link voltage performance will also be illustrated by implementing the DC link voltage controller. TABLE 3.1 shows the system parameters simulated in this part, and the control system parameters are the same with previous test (TABLE 3.2). The results are illustrated in Figs. 3.22 to 3.30. This simulation test is divided into four intervals. In following, these intervals are explained in detail.

At the beginning of simulation (t=0.1). DC link capacitor is charged to 800V,during $0.1 < t < 0.2$, external active power is not going through DC link ($i_{ext} = 0 \Rightarrow P_{ref} = 0$). At $t = 0.2s,\ 20kW$ active power is injected to the DC link(Fig.3.26), DC link controller regulates DC voltage following the reference voltage at 800V(until now, grid voltage is balanced). From 0.3s, a single load is connected to PCC($R = 18\Omega$) , resulting in voltage unbalance at PCC. Meanwhile, the proposed controller is applied to control the grid-connected DG inverter.it should be noted in this simulation $\left|i_{ref}^{-}\right|$ is fixed at $9A$. At 0.3s DG is sending active and reactive power with parameter of k_1 and k_2 both equal to 1 (Figs.3.22 and 3.23). As seen from Fig.3.23, the negative sequence of DG output current is equal to zero as expected (Eq. (3.13)). In this interval, PCC voltage negative sequence is 10V (Fig.3.16) with peak active power oscillation of 2000W (Fig.3.27).

During $0.5 < t < 0.7$, the injection of negative sequence current is initiated for PCC negative sequence voltage reduction using the proposed optimization method. However, during this interval, the maximum active power oscillation has been considered for evaluating the worth case scenario in optimization problem. Using this method, k_1 and k_2 are set on 0.994 and 1.006, respectively (Fig. 3.22 and 3.23), and DG injects $9A$ negative sequence of current (Fig.3.24) to decrease the

PCC negative sequence of voltage from $10V$ to $9.5V$ (Fig.3.25). In this interval, peak active power oscillation rises to $4000W$ (Fig. 3.27) because of non-optimum operation condition.

During $0.7 < t < 0.9$, optimum operation point is chosen to inject negative sequence of current for reducing PCC negative sequence voltage. Using this method, k_1 and k_2 are set on 1.0038 and 0.9965, respectively (Fig. 3.22 and 3.23), and the PCC negative sequence of voltage is reduced from $9.5V$ to $5.7V$ (Fig.3.25) by the same amount of DG negative sequence current ($9A$) injection (Fig. 3.24). Moreover, active power oscillation reduced to 2200W (Fig. 18). Considering Fig3.24 and Fig.3.25, the voltage unbalance factor drops from 9% to 6.5%, and the active power oscillation drops by 54% using optimization method. Considering these amount of reduction in voltage unbalance factor and active power oscillation, it can be concluded that if multiple DGs are connected to the grid, negative sequence voltage could drops to the range of 5%. Thanks to the notch filter function of DC link controller, DC link voltage(Fig.3.29) has some small ripples around 800V during these conditions, which does not cause the active power reference to be oscillatory (Fig.3.30).

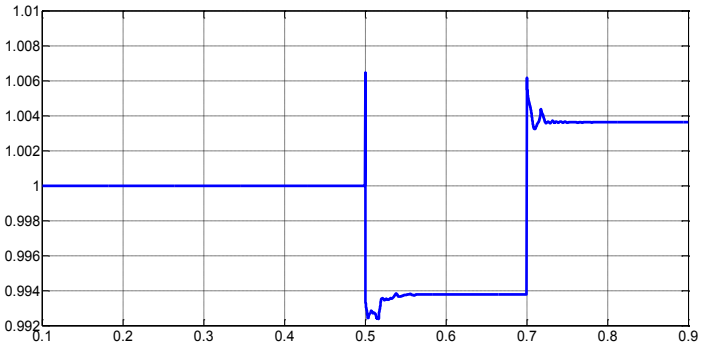

Fig.3. 22 Parameter of $k1$ in test 2.

(X-axis: time (s), Y-axis: value of $k1$)

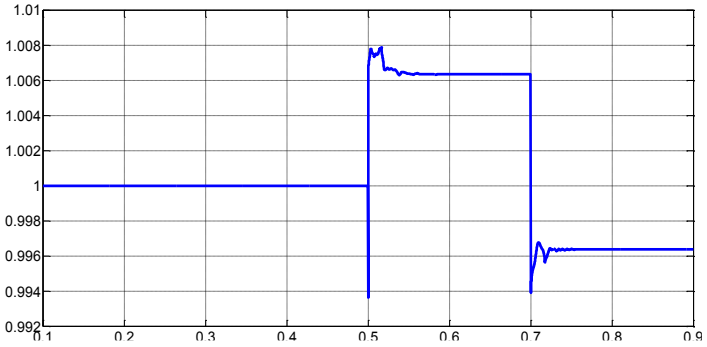

Fig.3. 23Parameter of $k2$ in test 2.

(X-axis: time (s), Y-axis: value of $k2$)

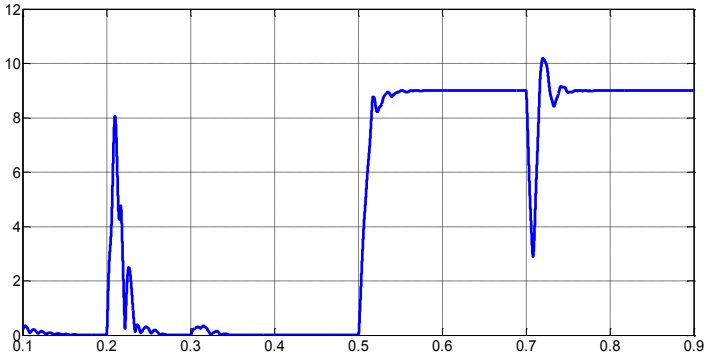

Fig.3. 24Generated negative sequence of DG current in test 2.

(X-axis: time (s), Y-axis: negative sequence current of DG (A))

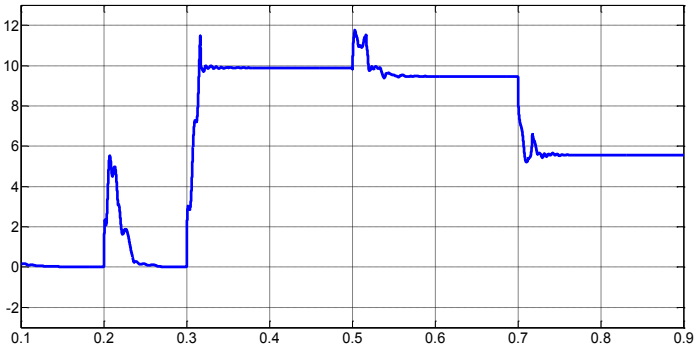

Fig.3. 25Negative sequence of voltage at PCC in test 2.

(X-axis: time (s), Y-axis: negative sequence voltage at PCC (V))

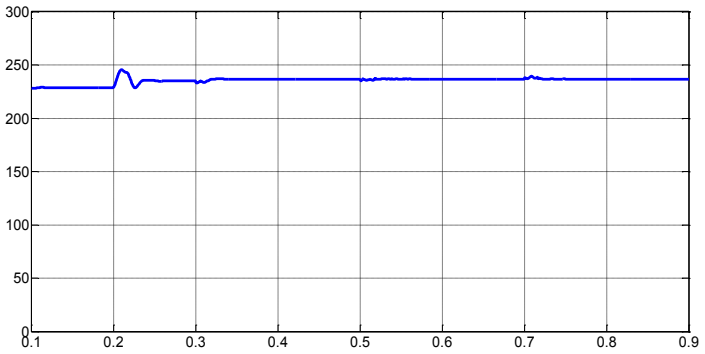

Fig.3. 26Positive sequence of voltage at PCC in test 2.

(X-axis: time (s), Y-axis: positive sequence voltage at PCC (V))

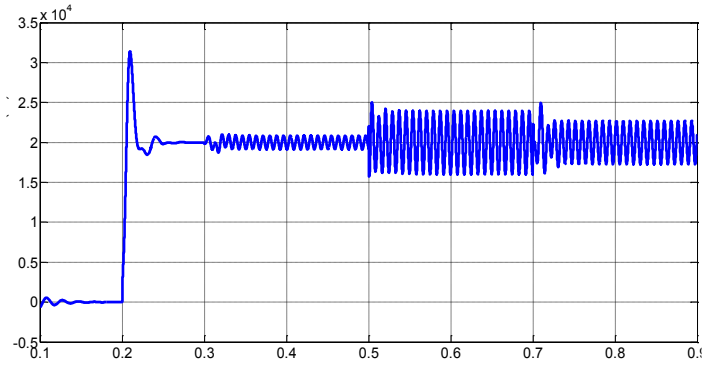

Fig.3. 27 Active power oscillation in test 2.

(X-axis: time (s), Y-axis: active power oscillation(W))

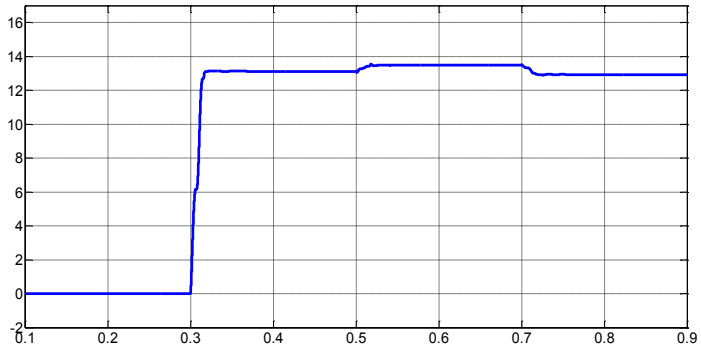

Fig.3. 28 Negative sequence of current going through single load in test 2.

(X-axis: time (s), Y-axis: negative sequence current of sing load (A))

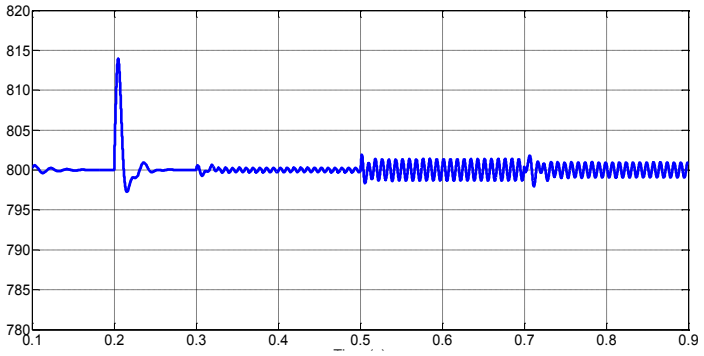

Fig.3. 29:DC link Voltage in test 2.

(X-axis: time (s), Y-axis: DC link voltage oscillation (V))

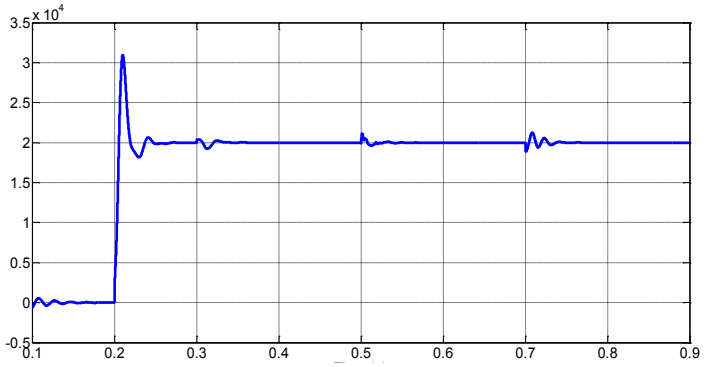

Fig.3. 30Active power reference produced by DC link voltage control

(X-axis: time (s), Y-axis: control ouput voltage (V))

3.7.3 Simulation results of sequence voltage detection

A case of detecting positive and negative sequence components in an unbalanced grid situation is simulated using MATLAB. In this method the gain of DSOGI-QSG is set at $k = \sqrt{2}$, Fig.3.31-Fig.3.36 shows the response of voltage sequence detector under unbalanced voltage. Unbalanced load is connected at PCC between 0.2s and 0.3s. Fig.3.31 shows the unbalanced voltage of Vabc, and estimated positive sequence voltage is shown in Fig.3.32 in $\alpha\beta$ reference frame. Meanwhile, the negative sequence voltage is detected in Fig.3.33 in $\alpha\beta$ reference frame as well. Fig.3.34 and Fig.3.35 shows the estimated amplitude for positive and negative sequence voltage v^+ and v^-, finally, the positive seuqence phase angle is shown in Fig.3.36. these waveforms are calculated as follows:

$$|v^+| = \sqrt{(v_\alpha^+)^2 + \left(v_\beta^+\right)^2}\ ,\ |v^-| = \sqrt{(v_\alpha^-)^2 + \left(v_\beta^-\right)^2},\ \theta^+ = tan^{-1}\frac{v_\beta^+}{v_\alpha^+} \tag{3-60}$$

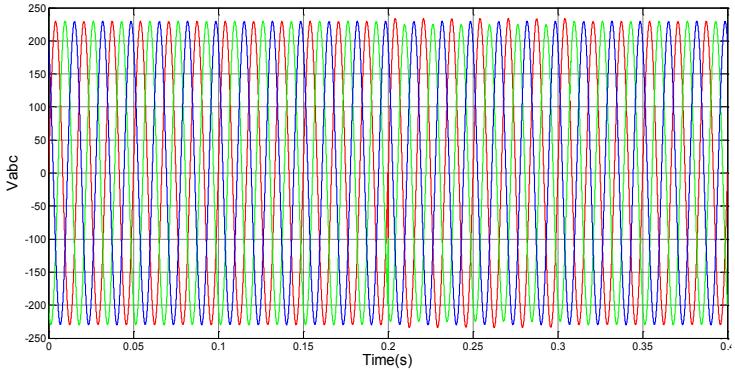

Fig.3. 31 Voltage at DG terminal in the situation of voltage unbalance

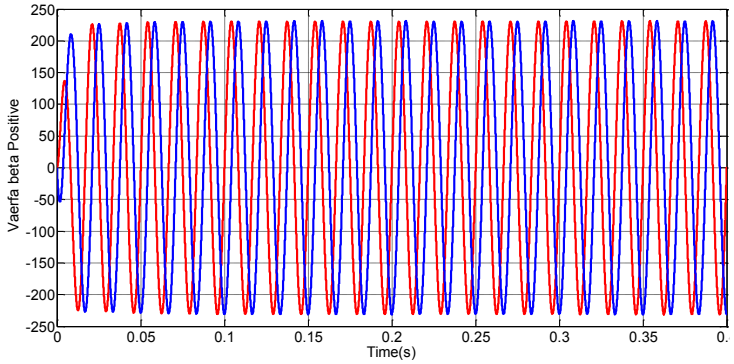

Fig.3. 32Detection of sine wave positive sequence voltage

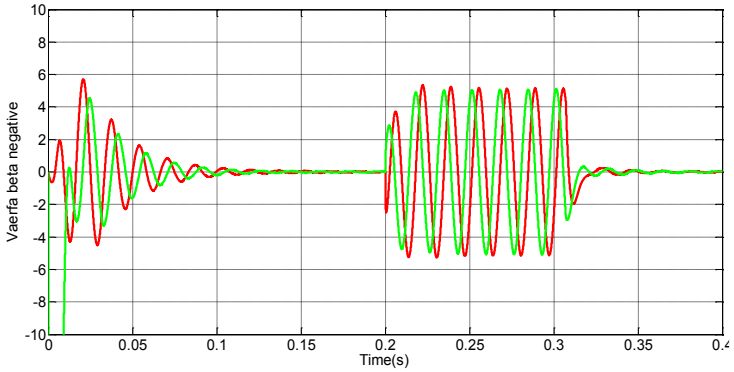

Fig.3. 33Detection of sine wave negative sequence voltage

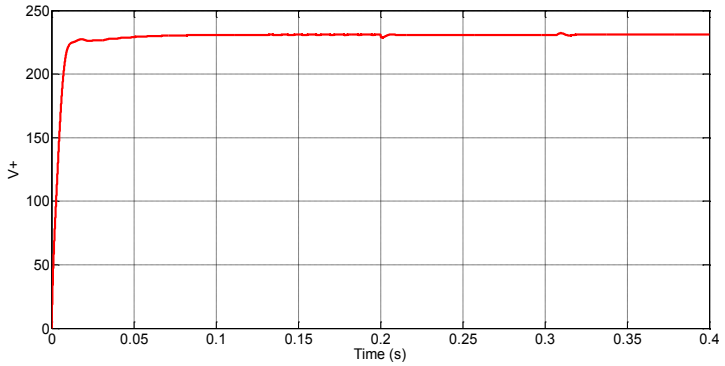

Fig.3. 34Amplitude of positive sequence voltage

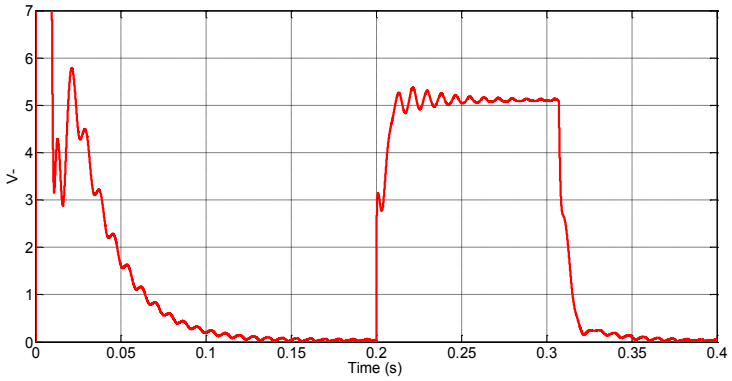

Fig.3. 35Amplitude of negative sequence voltage

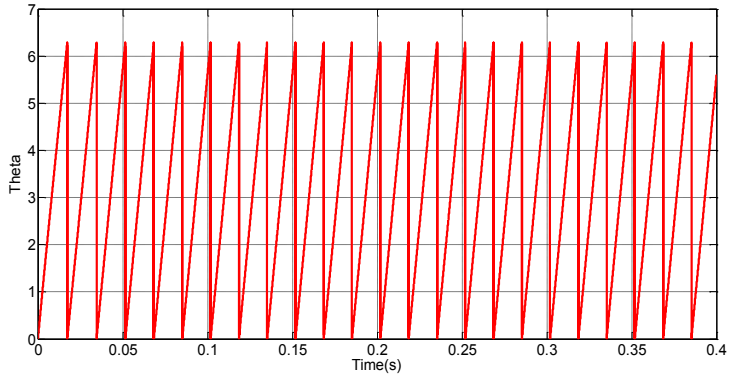

Fig.3. 36 Phase angle of positive sequence voltage

3.8 Summary

Two separate control schemes have been proposed for three phase DG inverter

under single load unbalance. Cancellation of active power oscillation strategy was first proposed Implementing this strategy, active power oscillation can be fully cancelled out with the negative sequence voltage dropping at PCC. Then the strategy for reduction of negative sequence voltage was proposed, where it can greatly reduce negative sequence voltage and ease active power oscillation. Simulation results have been used to verify the effectiveness of the proposed scheme, analysis was present to explain the phenomena in the simulation. Finally, effectiveness of extracting positive sequence and negative sequence voltage in PLL was illustrated in the chapter.

Chapter 4 Experiment Results

The control strategies presented in Chapter2 and Chapter 3 are tested in laboratory prototype, where a three phase voltage source converter including LCL filter are used connecting to a weak grid though an inductance (L=5mH), the grid is replaced by a programmable three phase ac power source. The real time code for experiment is generated by dSpace1103 (Fig.4.1). In order to create the unbalanced voltage situation, three phase unbalanced loads are connected at PCC.

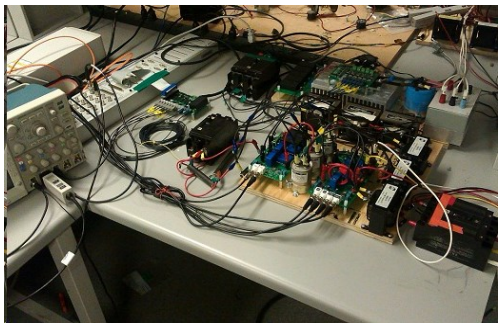

Fig.4. 1 Photo of dSPACE experiemntal platform

4. 1 Experimental results of flexible control strategies under voltage unbalance

Details of the parameter is shown in TABLE 4.1. In the experiment, the DC link voltage is provided by a constant dc voltage source. But this does not affect observation of performance of different methods, as DG output real and reactive power are measured. In order to validate the aforementioned flexible control strategies, the balanced ac power source has been programmed to produce the voltage at the terminal of PCC. Three unbalanced load are connected at the PCC to generate unbalanced voltage shown in Fig.4.2 . In the following, the grid current and output power waveforms are illustrated for each control strategies.

TABLE 4. 1Experiment Parameter of flexible operation

	Symbol	Value
DC link voltage	v_{dc}	150V
Inverter side inductor	L_i	2.5mH
Capacitor	C	$50\mu F$
Grid side inductor	L_g	2.5mH
Resistance in series with Capacitor	R_C	1Ω
Three phase unbalanced Load	$R_1 - R_2 - R_3$	3-5-9Ω
Grid voltage(Phase to Ground)	v_g(RMS)	30V
Active power reference	P^*	100W
Reactive power reference	Q^*	0Var

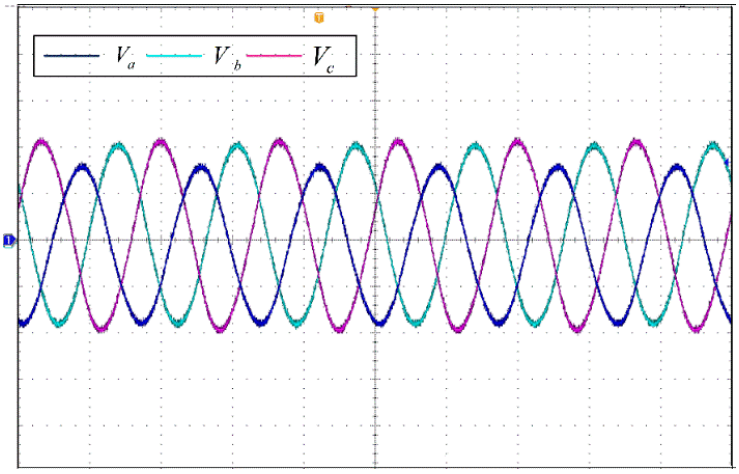

Fig.4. 2 Unbalanced Voltage at PCC(X-axis_time: 2ms/div, Y-axis_PCC Voltage 20V/div)

4.1.1 Instantaneous Active Reactive Control (IARC)

The current waveform and output active and reactive powers for this control strategy are depicted in Fig.4.3 and Fig.4.4, respectively. As noticed, current waveform is distorted in order to satisfy the demand of unity power factor control in the unbalanced voltage situation.

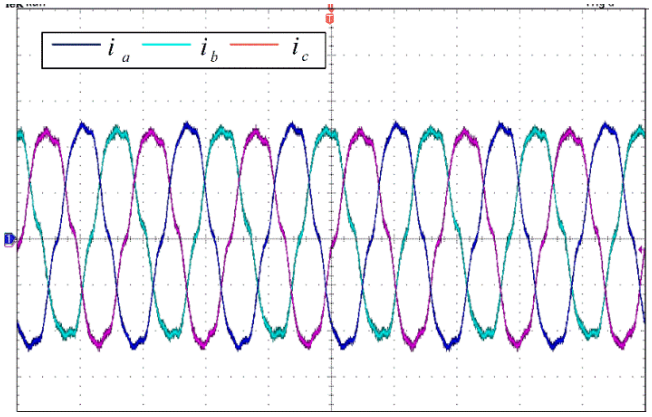

Fig.4. 3grid current using IARC strategy

(X-axis_time: 2ms/div, Y-axis_current:1A/div)

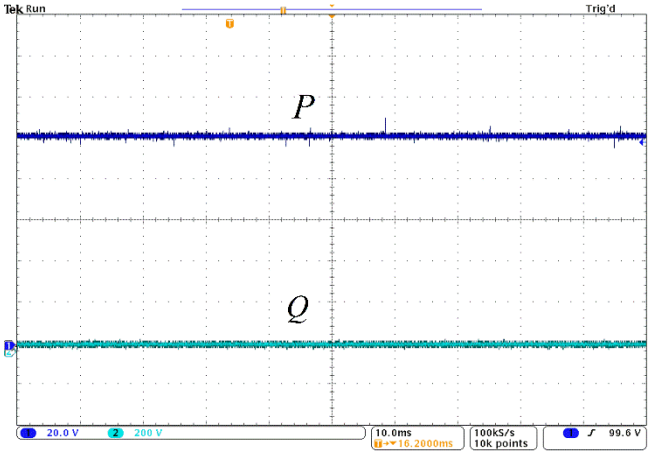

Fig.4. 4Instantaneous active and reactive power using IARC strategy

(X-axis_time:1ms/div, Y-axis_power:20W/div)

4.1.2 Positive-Negative Sequence Control (PNSC)

Fig.4.5 and Fig.4.6 show the grid current and active and reactive power that delivered to the utility when this control strategy is used. This control strategy is to inject negative sequence current in order to cancel the oscillation in active power. As shown in Fig.4.5 no active power oscillation exists in the PCC.

The grid current is unbalanced, exhibiting double the fundamental frequency harmonic. The disadvantage of this control strategy is large oscillation in the reactive power due to the interaction between negative sequence active current with the positive sequence voltage and the positive sequence active current with the

negative sequence voltage.

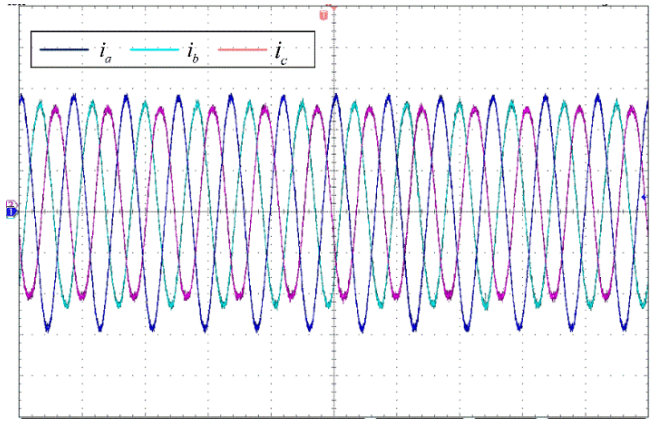

Fig.4. 5 grid current using PNSC strategy

(X-axis_time: 2ms/div, Y-axis_current:1A/div)

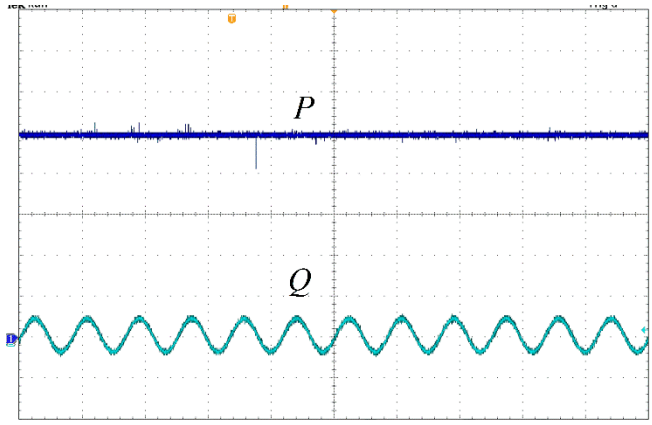

Fig.4. 6Instantaneous active and reactive power using PNSC strategy

(X-axis_time:1ms/div, Y-axis_power:20W/div)

4.1.3 Average Active Reactive Control (AARC)

In the AARC control strategy, reactive power has no oscillation, but active power exhibits large oscillation at double the fundamental frequency due to the oscillation in the voltage, which is shown in Fig.4.8.

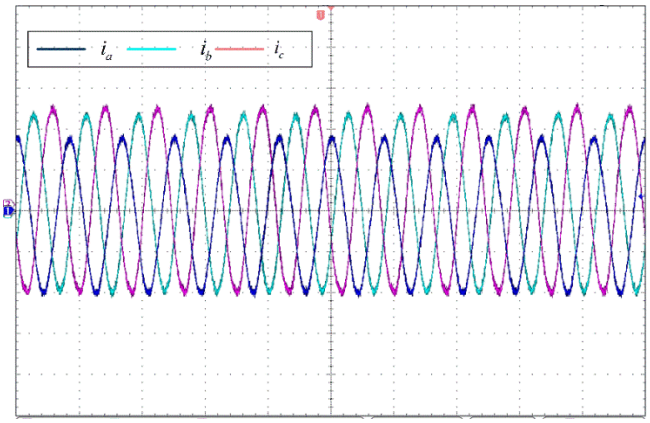

Fig.4. 7 grid current using AARC strategy

(X-axis_time: 2ms/div, Y-axis_current:1A/div)

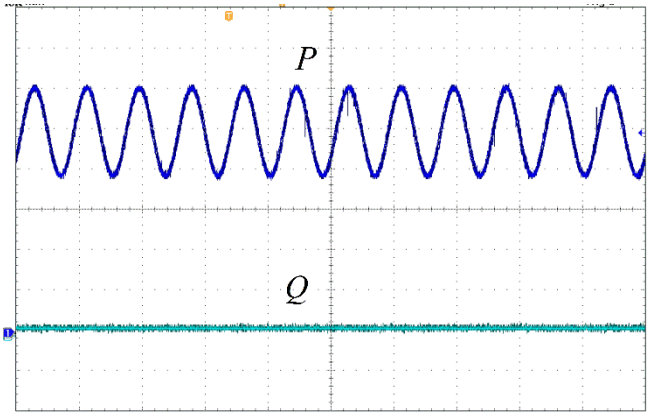

Fig.4. 8Instantaneous active and reactive power using AARC strategy

(X-axis_time:1ms/div, Y-axis_power:20W/div)

4.1.4 Balanced Positive-Sequence Control (BPSC)

Fig.4.9 and Fig.4.10 show the current and power waveforms in the case of BPSC control. As only the positive-sequence component of the grid voltage is used for calculating the grid current references, the current are sinusoidal and balanced, it can be observed that the active power and reactive both exhibit oscillation at twice fundamental frequency due to the interaction between the positive sequence current and negative sequence voltage.

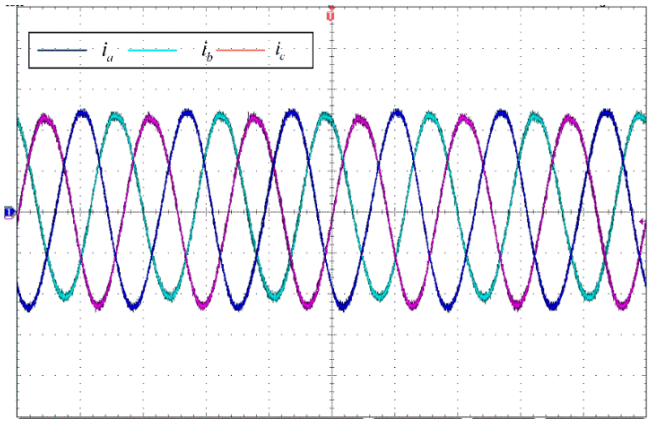

Fig.4. 9 grid current using BPSC strategy

(X-axis_time: 2ms/div, Y-axis_current:1A/div)

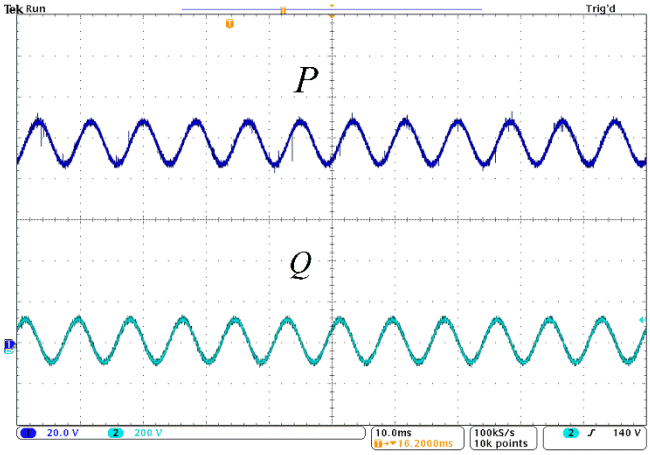

Fig.4. 10 Instantaneous active and reactive power using BPSC strategy

(X-axis_time:1ms/div, Y-axis_power:20W/div)

4.2 Experimental results of DG control strategies for voltage unbalance compensation

4.2.1 Cancellation of active power oscillation

In the experiment, the parameter of set-up is shown in TABLE 4.2. In this part of experiment, three phase Y-connected unbalanced load with 3-5-9Ω resistance is connected to the grid at PCC, and $330W$ average active power and $50Var$ average reactive power are delivered into the grid. The results are shown from

Fig.4.11 to Fig.4.18.

Before enabling the active power oscillation strategy (k1=1, k2=1), active power oscillation is around 30W(Fig.4.11). In this state, all the negative sequence current generated by three phase unbalanced loads goes through the line impedance. After using the control strategy at t=0.3s, active power oscillation drops to zero. Fig.4.12 shows the zoomed-in description of active power. Three phase unbalanced voltage at PCC is shown in Fig.4.13. Details of positive sequence voltage and negative sequence voltage are also illustrated in Fig.4.15 and Fig.4.16, from which it is easy to observe that negative sequence voltage drop from 4.7 to 3.8 and positive sequence voltage keep constant. Current before initializing the control strategy is fully sinusoidal due to only positive sequence current injecting, while is unbalanced after implementing new control strategy. Fig.4.16 and Fig. 4.17 show the change of k1 and k2 and zoomed one.

TABLE 4. 2 Experiment Parameter of active power oscillation cancellation

	Symbol	Value
DC link voltage	v_{dc}	150V
Inverter side inductor	L_i	2.5mH
Capacitor	C	$50\mu F$
Grid side inductor	L_g	2.5mH
Resistance in series with Capacitor	R_C	1Ω
Three phase unbalanced Load	$R_1 - R_2 - R_3$	3-5-9Ω
Grid voltage(Phase to Ground)	v_g(RMS)	30V
Average active power	P	330W
Average reactive power	Q	50 Var

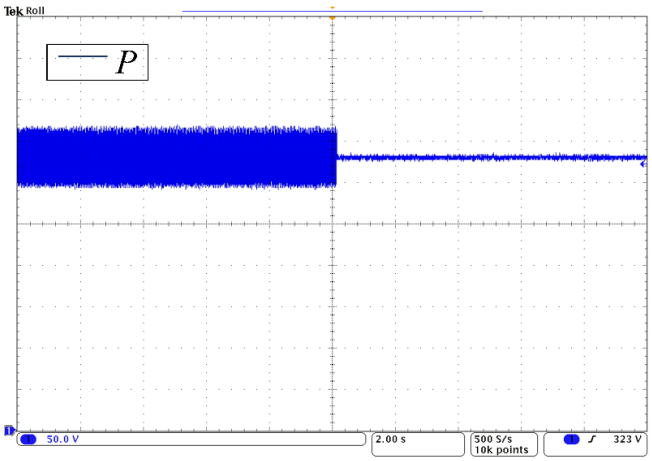

Fig.4. 11Instantaneous active power (X-axis: 2s/div Y-axis:50W/div)

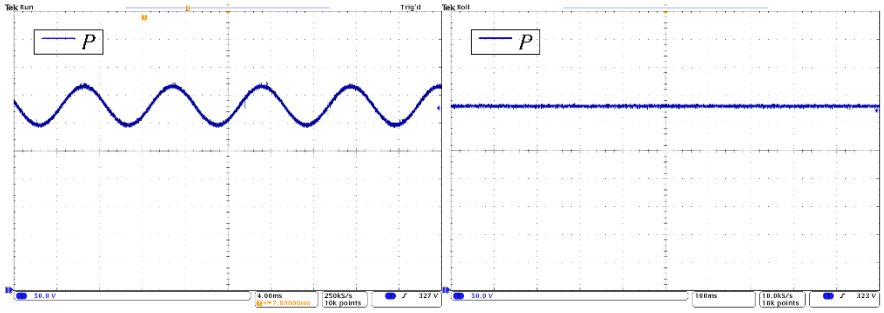

(a) (b)

Fig.4. 12Zoomed-in active power before and after using the active power cancellation strategy

(Y-axis:50W/div)

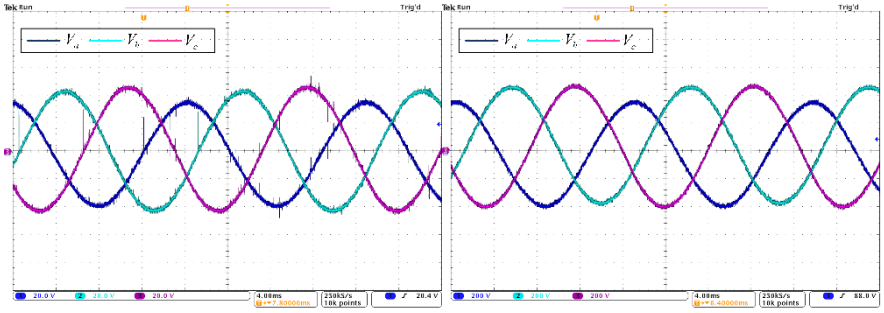

(a) (b)

Fig.4. 13Voltage at PCC before and after using the strategy

(X-axis: 4ms/div Y-axis:20V/div)

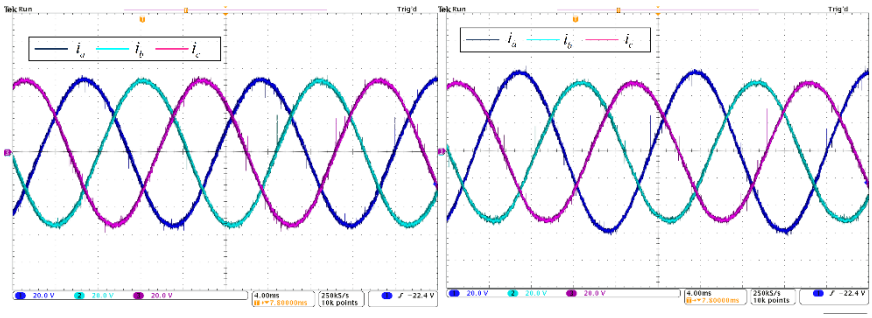

(a) (b)

Fig.4. 14current injecting into PCC before and after using the strategy

(X-axis: 4ms/div Y-axis:2A/div)

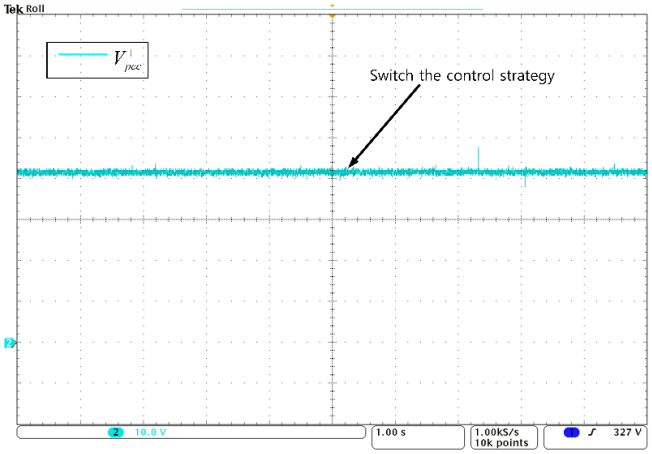

Fig.4. 15Positive sequence voltage at PCC (X-axis: 1s/div Y-axis:10V/div)

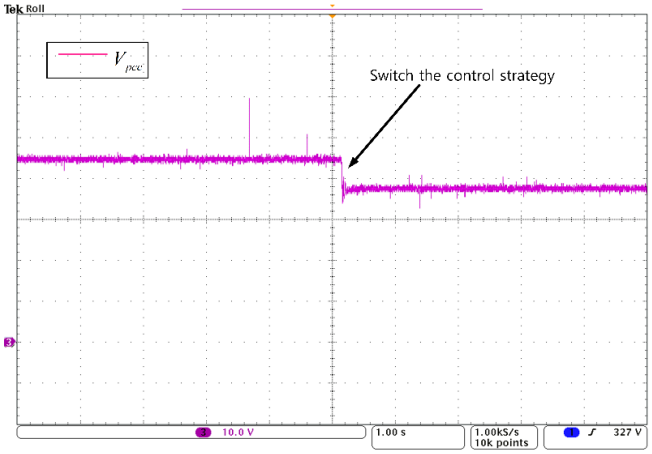

Fig.4. 16Negative sequence voltage at PCC (X-axis: 1s/div Y-axis:1V/div)

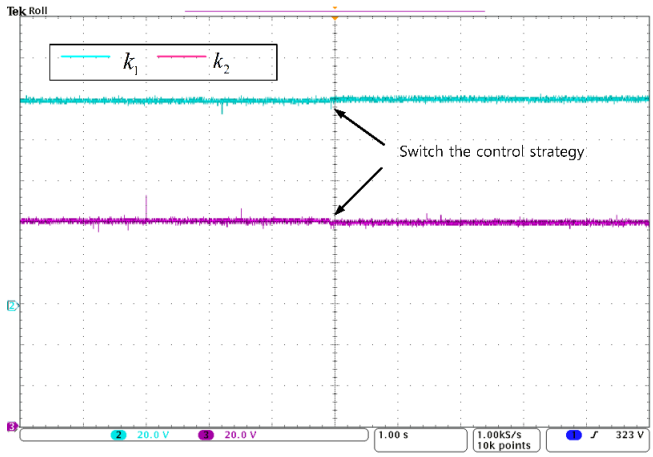

Fig.4. 17 k1 and k2 before and after using the control strategy

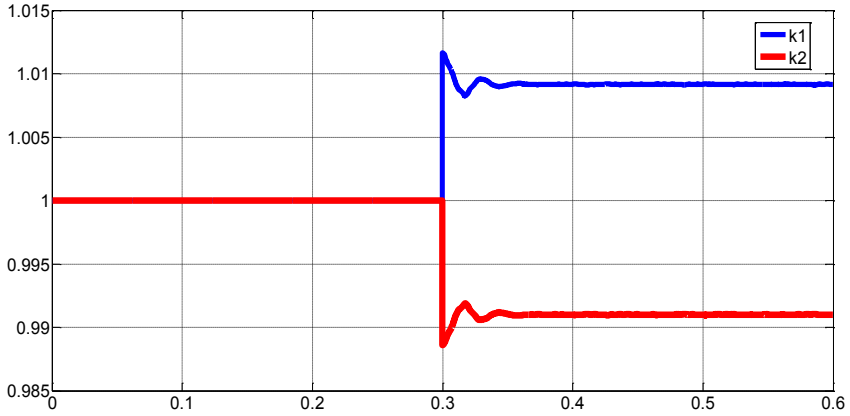

Fig.4. 18 zoomed k1 and k2

4.2.2 Negative sequence voltage reduction

In the experiment, the parameter of set-up is the same and shown in TABLE.4.2. Only optimal control strategy is shown in the experiment, because in the real control strategy, the worst case will not be considered. Before initializing the optimal control strategy at $k1 = 1$ and $k2 = 1$, DG active power oscillation is around 30W (Fig.4.19). In this scenario, all the negative sequence current generated by three phase unbalanced loads goes through the line impedance. After using the optimal control strategy, DG active power oscillation increased a little bit due to injection of negative sequence current from DG. Fig.4.20 shows the zoomed-in description of active power. Three phase unbalanced voltage at PCC is shown in

Fig.4.21. Details of positive sequence voltage and negative sequence voltage are also illustrated in Fig.4.23 and Fig.4.24, from which it is easy to observe that negative sequence voltage drop from 4.7 to 3.2 and positive sequence voltage keep constant, making the voltage unbalance factor drops from 11% to 7%. DG output current before using the control strategy is fully sinusoidal as only positive sequence current is injected. While it is unbalanced after implementing the proposed control strategy(Fig.4.22). Fig.4.23 and Fig. 4.24 show the change of $k1$ and $k2$ and zoomed one (from $k1$=1 and $k2$=1 to $k1$=1.012 and $k2$=0.9884).

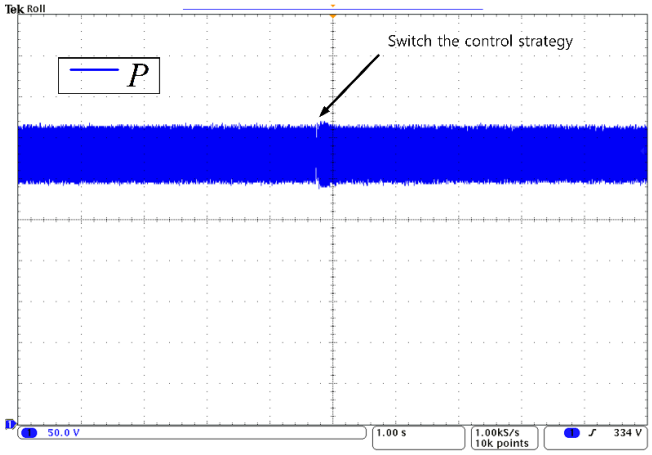

Fig.4. 19 Instantaneous active power at PCC (X-axis:1s/div Y-axis:50W/div)

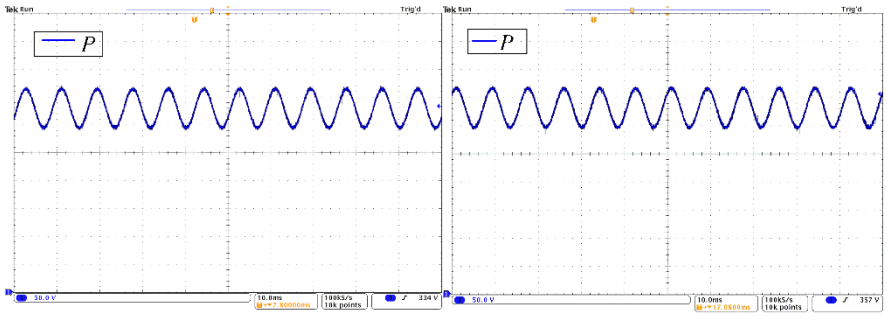

(a) (b)

Fig.4. 20 Zoomed-in active power before and after using the strategy

(Y-axis:50W/div)

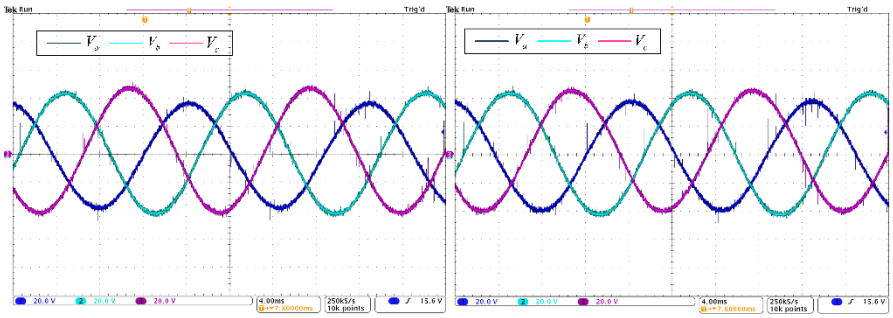

(a) (b)

Fig.4. 21 Voltage at PCC before and after using the strategy

(X-axis: 4ms/div Y-axis:20V/div)

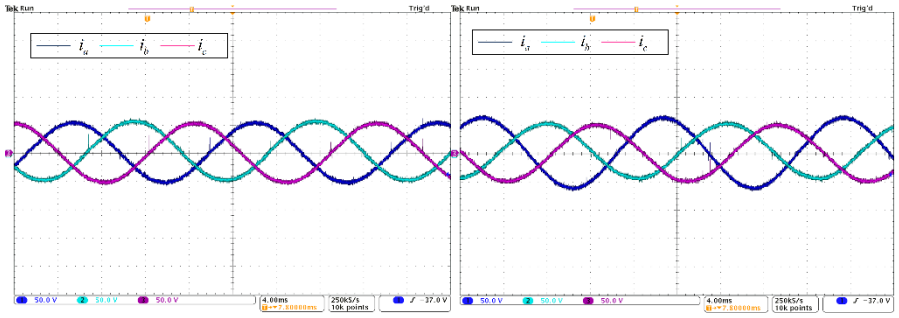

(a) (b)

Fig.4. 22 Current injecting into grid before and after using the strategy

(X-axis: 4ms/div Y-axis:5A/div)

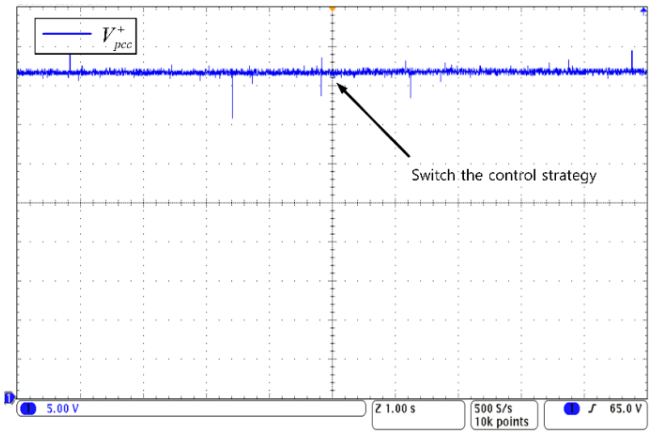

Fig.4. 23 Positive sequence voltage at PCC(X-axis: 1s/div Y-axis:5V/div)

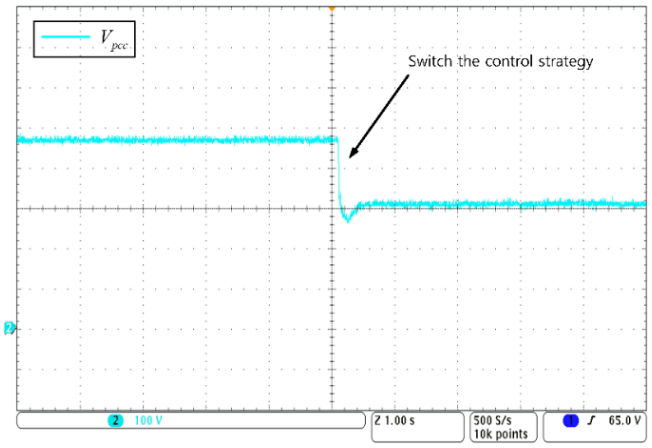

Fig.4. 24 Negative sequence voltage at PCC(X-axis: 1s/div Y-axis:1V/div)

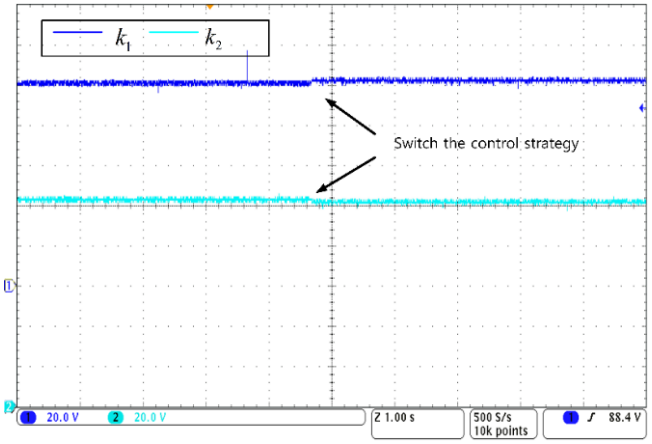

Fig.4. 25 k1 and k2 before and after using the control strategy

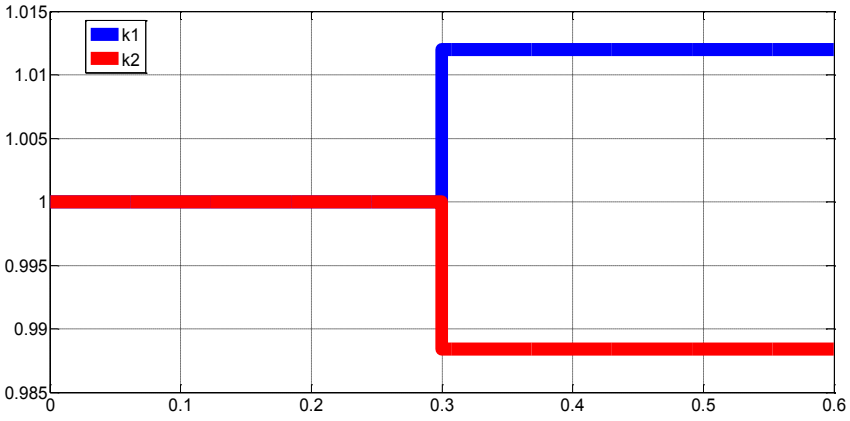

Fig.4. 26 zoomed k1 and k2

4.3 Summary

In this chapter, flexible DG control strategy under unbalanced voltage is reviewed in Chapter 2 and the two proposed control strategy for unbalanced voltage compensation in Chapter 3 have been verified in the laboratory prototype. Specifically, at the first part, different control strategies to generate current reference have been carried out in the experiment, in order to manage active power and reactive power oscillation. Experimental results is fully in agreement with the simulation results. In the second part, the two proposed methods to alleviate grid voltage unbalance and minimize active power are carried out in the prototype. Results of waveforms verified the effectiveness of the simulation results.

Chapter 5 Conclusion and Future work

5.1 Conclusion

In the past few years, renewable energy such as wind and solar, known as DGs, has been emerging as an alternative energy resource in the world, where power electronic converters are used as interfaces to convert their output voltages to the grid compatible AC voltages. Meanwhile, techniques for controlling power electronic interfaced DGs face a lot of challenges, especially when voltage unbalance problems occur. Since voltage unbalance issues result in various serious problems, such as electrical machine overheating, transformer overloading, and capacity limitation of power electronics devices, literatures have investigated how to ease the voltage unbalance issues.

This thesis first reviewed the flexible control strategy of grid-interfacing converters in unbalanced voltage situation, the results of analysis was guideline for design of a flexible active power controller which was capable of adapting itself to unbalanced grid. Specifically, it was possible to transfer active and reactive power without oscillation at PCC at the expense of injecting highly distorted current using IARC control strategy. Moreover, constant active power transfer was achieved by implementing the PNSC control strategy at the expense of generating reactive power oscillation through decomposing current reference into positive and negative sequence ones. Furthermore, reactive power kept constant using AARC control strategy if DG operated as STATCOM. However, active power oscillation was the drawback of this control strategy. Finally, a tradeoff solution (BPSC) allowed for sinusoidal current injection with the active power and reactive power oscillation. Overall, it was proven that DG is able to work flexibly depending on grid regulator under unbalanced voltage.

Moreover, in Chapter 3 two control strategies for voltage unbalance compensation while minimization of active power in the presence of DGs under load unbalance conditions have been proposed. First, cancellation of active power oscillation strategy was proposed where the negative sequence of PCC voltage can be reduced as a by-product. However, this method cannot directly control the DG's negative sequence current and therefore the negative sequence voltage compensation level cannot be adjusted. On the other hand, the second method could minimize the active power oscillation and compensate the negative sequence voltage at PCC with adjustable DG negative sequence reference current. By using this method, negative sequence voltage at PCC was alleviated and DC link voltage oscillation was smoothed, leading to enhancement of power quality in the grid and stabilization of grid-interfacing converter.

Finally, all the studied method in Chapter 2 and Chapter 3 have been verified by experiment in the DG prototype. Compared to the simulation results in Chapter 2 and Chapter 3, the experiment results were highly accordant with their counterparts in the simulation.

5.2 Future Work

There are some areas where future work can focus on.

First, stability issue of the control strategy in optimized mode should be analyzed due to instability problem existing in the control system caused by high value of negative sequence current injection. Some researchers have studied the stability issues when converter is modeled by a positive and negative sequence impedance [50]. It is suggested that the stability issue existing in our system can be investigated by reviewing those reference first.

Second, due to the capability limitation of injecting negative sequence current

of single DG, multiple DGs working coordinately to compensate the negative sequence voltage is the next step of study both in grid-interfacing mode and islanded mode. Hierarchical control methods to coordinate multiple DG have been developed in recent years. How to design each level controller greatly impact the overall performance of unbalanced voltage compensation.

Third, reactive power oscillation and its effects on DG and PCC in the grid should be investigated as well. As reactive power can provide voltage support function at PCC, it is possible to flexibly regulate the reactive power by modifying the reference generation.

Finally, this thesis only focuses on negative sequence voltage compensation of DG system. It is also possible to provide other power quality enhancement service such as harmonic compensation of distribution system and reactive power support function.

Reference

[1] W. Fei, "Flexible Operation of Grid-Interfacing Converters in Distribution Networks: Bottom-up Solutions to Voltage Quality Enhancement," Ph.D, Eindhoven University of Technology 2010.

[2] Y. L. Bin Wu, Navid Zrgari, *Power conversion and control of wind energy systems*: wiley, 2010.

[3] H. Jinwei, L. Yun Wei, and M. S. Munir, "A Flexible Harmonic Control Approach Through Voltage-Controlled DG and Grid Interfacing Converters," *Industrial Electronics, IEEE Transactions on,* vol. 59, pp. 444-455, 2012.

[4] M. H. J. Bollen, *UNDERSTANDING POWER QUALITY PROBLEMS Voltage Sags and Interruptions*, 2000.

[5] A. von Jouanne and B. Banerjee, "Assessment of voltage unbalance," *Power Delivery, IEEE Transactions on,* vol. 16, pp. 782-790, 2001.

[6] A. v. J. a. B. B. Banerjee, "Voltage unbalance: Power quality issues, related standards and mitigation techniques," *Electric Power Research Institute,* 2000.

[7] T. E. Seiphetlho and A. P. J. Rens, "On the assessment of voltage unbalance," in *Harmonics and Quality of Power (ICHQP), 2010 14th International Conference on*, 2010, pp. 1-6.

[8] J. D. Kneck, D. A. Casada, and P. J. Otaduy, "A comparison of two energy efficient motors," *Energy Conversion, IEEE Transactions on,* vol. 13, pp. 140-147, 1998.

[9] L. Tzung-Lin, H. Shang-Hung, and C. Yu-Hung, "D-STATCOM With Positive-Sequence Admittance and Negative-Sequence Conductance to Mitigate Voltage Fluctuations in High-Level Penetration of Distributed-Generation Systems," *Industrial Electronics, IEEE Transactions on,* vol. 60, pp. 1417-1428, 2013.

[10] D. Boroyevich, I. Cvetkovic, D. Dong, R. Burgos, W. Fei, and F. Lee, "Future electronic power distribution systems a contemplative view," in *Optimization of Electrical and Electronic Equipment (OPTIM), 2010 12th International Conference on*, 2010, pp. 1369-1380.

[11] U. Jayatunga, S. Perera, and P. Ciufo, "Impact of mains connected three-phase induction motor loading levels on network voltage unbalance attenuation," in *Power System Technology (POWERCON), 2012 IEEE International Conference on*, 2012, pp. 1-6.

[12] "Motor and Generators," *NEMA Standards Publication no.MG 1-1993*.

[13] M. F. M. R.C. Dugan, and H.W, "Electrical Power Systems Quality," *New*

York: McGraw-Hill, 1996.

[14] A. C. 1995, " American national standard for electric power systems and equipment," 1995.

[15] E. P. E. A. Center, "Input performance of ASDs during supply voltage unbalance,," *Power quality testing network PQTN Brief no. 28,* 1996.

[16] N. Standards, "NEMA Standards Publication MG 1-1998(Revision 3, 2002) Interfiled," 2002.

[17] "IEEE Standard for Interconnecting Distributed Resources With Electric Power Systems," *IEEE Std. 1547.2-2008,* 2008.

[18] A. Cziker, M. Chindris, and A. Miron, "Voltage unbalance mitigation using a distributed generator," in *Optimization of Electrical and Electronic Equipment, 2008. OPTIM 2008. 11th International Conference on*, 2008, pp. 221-226.

[19] EPRI, "Voltage Unbalance: Power Quality Issues,Related Standards and Mitigation Techniques," 2008.

[20] D. R. Smith, H. R. Braunstein, and J. D. Borst, "Voltage unbalance in 3- and 4-wire delta secondary systems," *Power Delivery, IEEE Transactions on,* vol. 3, pp. 733-741, 1988.

[21] P. Salmeron and R. S. Herrera, "Distorted and unbalanced systems compensation within instantaneous reactive power framework," *Power Delivery, IEEE Transactions on,* vol. 21, pp. 1655-1662, 2006.

[22] D. Graovac, V. Katic, and A. Rufer, "Power Quality Problems Compensation With Universal Power Quality Conditioning System," *Power Delivery, IEEE Transactions on,* vol. 22, pp. 968-976, 2007.

[23] T. Ackermann, G. Andersson, and L. Söder, "Distributed generation: a definition," *Electric Power Systems Research,* vol. 57, pp. 195-204, 4/20/ 2001.

[24] L. F. a. D. Infield, "Renewable energy in power systems," *Wiley,* 2008.

[25] A. Timbus, M. Liserre, R. Teodorescu, P. Rodriguez, and F. Blaabjerg, "Evaluation of Current Controllers for Distributed Power Generation Systems," *Power Electronics, IEEE Transactions on,* vol. 24, pp. 654-664, 2009.

[26] F. Blaabjerg, R. Teodorescu, M. Liserre, and A. V. Timbus, "Overview of Control and Grid Synchronization for Distributed Power Generation Systems," *Industrial Electronics, IEEE Transactions on,* vol. 53, pp. 1398-1409, 2006.

[27] H. Jinwei, L. Yun Wei, F. Blaabjerg, and W. Xiongfei, "Active Harmonic Filtering Using Current-Controlled, Grid-Connected DG Units With Closed-Loop Power Control," *Power Electronics, IEEE Transactions on,* vol. 29, pp. 642-653, 2014.

[28] M. Hojo, Y. Iwase, T. Funabashi, and Y. Ueda, "A method of three-phase

balancing in microgrid by photovoltaic generation systems," in *Power Electronics and Motion Control Conference, 2008. EPE-PEMC 2008. 13th*, 2008, pp. 2487-2491.

[29] C. Po-Tai, C. Chien-An, L. Tzung-Lin, and K. Shen-Yuan, "A Cooperative Unbalance Compensation Method for Distributed Generation Interface Converters," in *Industry Applications Conference, 2007. 42nd IAS Annual Meeting. Conference Record of the 2007 IEEE*, 2007, pp. 1567-1573.

[30] M. B. Delghavi and A. Yazdani, "Islanded-Mode Control of Electronically Coupled Distributed-Resource Units Under Unbalanced and Nonlinear Load Conditions," *Power Delivery, IEEE Transactions on,* vol. 26, pp. 661-673, 2011.

[31] M. Savaghebi, A. Jalilian, J. C. Vasquez, and J. M. Guerrero, "Secondary Control for Voltage Quality Enhancement in Microgrids," *Smart Grid, IEEE Transactions on,* vol. 3, pp. 1893-1902, 2012.

[32] G. S. Kumar, B. K. Kumar, and M. K. Mishra, "Mitigation of voltage unbalances and sags with phase-jumps in grid connected wind generation," in *Renewable Power Generation (RPG 2011), IET Conference on*, 2011, pp. 1-6.

[33] H. Jinwei, M. S. Munir, and L. Yun Wei, "Opportunities for power quality improvement through DG-grid interfacing converters," in *Power Electronics Conference (IPEC), 2010 International*, 2010, pp. 1657-1664.

[34] Y. A. R. I. Mohamed, "Mitigation of Dynamic, Unbalanced, and Harmonic Voltage Disturbances Using Grid-Connected Inverters With LCL Filter," *Industrial Electronics, IEEE Transactions on,* vol. 58, pp. 3914-3924, 2011.

[35] W. Feng, Z. Xinan, D. M. Vilathgamuwa, C. San Shing, and W. Shuai, "Mitigation of distorted and unbalanced stator voltage of stand-alone doubly fed induction generators using repetitive control technique," *Electric Power Applications, IET,* vol. 7, pp. 654-663, 2013.

[36] R. I. Amirnaser Yazdani, *Voltage-Sourced Converter in Power Systems*: IEEE Wiley, 2010.

[37] H. Akagi, Y. Kanazawa, and A. Nabae, "Instantaneous Reactive Power Compensators Comprising Switching Devices without Energy Storage Components," *Industry Applications, IEEE Transactions on,* vol. IA-20, pp. 625-630, 1984.

[38] P. Rodriguez, A. V. Timbus, R. Teodorescu, M. Liserre, and F. Blaabjerg, "Flexible Active Power Control of Distributed Power Generation Systems During Grid Faults," *Industrial Electronics, IEEE Transactions on,* vol. 54, pp. 2583-2592, 2007.

[39] M. L. Remus Teodorescu, Pedro Rodr´ıguez, "GRID CONVERTERS FOR PHOTOVOLTAIC AND WIND POWER SYSTEMS," *IEEE Wiley,* 2008.

[40] P. Rodriguez, A. V. Timbus, R. Teodorescu, M. Liserre, and F. Blaabjerg,

"Independent PQ Control for Distributed Power Generation Systems under Grid Faults," in *IEEE Industrial Electronics, IECON 2006 - 32nd Annual Conference on*, 2006, pp. 5185-5190.

[41] W. Fei, J. L. Duarte, and M. A. M. Hendrix, "Pliant Active and Reactive Power Control for Grid-Interactive Converters Under Unbalanced Voltage Dips," *Power Electronics, IEEE Transactions on,* vol. 26, pp. 1511-1521, 2011.

[42] P. Rodriguez, A. Luna, J. R. Hermoso, I. Etxeberria-Otadui, R. Teodorescu, and F. Blaabjerg, "Current control method for distributed generation power generation plants under grid fault conditions," in *IECON 2011 - 37th Annual Conference on IEEE Industrial Electronics Society*, 2011, pp. 1262-1269.

[43] Rodri, x, P. guez, A. Luna, I. Candela, R. Mujal*, et al.*, "Multiresonant Frequency-Locked Loop for Grid Synchronization of Power Converters Under Distorted Grid Conditions," *Industrial Electronics, IEEE Transactions on,* vol. 58, pp. 127-138, 2011.

[44] F. L. Lewis, *optimal control*, 1986.

[45] A. Yazdani and R. Iravani, "An accurate model for the DC-side voltage control of the neutral point diode clamped converter," in *Power Engineering Society General Meeting, 2006. IEEE*, 2006, p. 1 pp.

[46] L. Asiminoaei, F. Blaabjerg, and S. Hansen, "Detection is key - Harmonic detection methods for active power filter applications," *Industry Applications Magazine, IEEE,* vol. 13, pp. 22-33, 2007.

[47] B. P. McGrath, D. G. Holmes, and J. J. H. Galloway, "Power converter line synchronization using a discrete Fourier transform (DFT) based on a variable sample rate," *Power Electronics, IEEE Transactions on,* vol. 20, pp. 877-884, 2005.

[48] W. Yi Fei and L. Yun Wei, "Three-Phase Cascaded Delayed Signal Cancellation PLL for Fast Selective Harmonic Detection," *Industrial Electronics, IEEE Transactions on,* vol. 60, pp. 1452-1463, 2013.

[49] P. Rodriguez, R. Teodorescu, I. Candela, A. V. Timbus, M. Liserre, and F. Blaabjerg, "New Positive-sequence Voltage Detector for Grid Synchronization of Power Converters under Faulty Grid Conditions," in *Power Electronics Specialists Conference, 2006. PESC '06. 37th IEEE*, 2006, pp. 1-7.

[50] M. Cespedes and S. Jian, "Impedance Modeling and Analysis of Grid-Connected Voltage-Source Converters," *Power Electronics, IEEE Transactions on,* vol. 29, pp. 1254-1261, 2014.